

PWM Control Scheme for Quasi-Switched-Boost Inverter to Improve Modulation Index

Fuad Munther Fuad Khawaja

Submitted to the
Institute of Graduate Studies and Research
in partial fulfillment of the requirements for the degree of

Master of Science
in
Electrical and Electronic Engineering

Eastern Mediterranean University
July 2019
Gazimağusa, North Cyprus

Approval of the Institute of Graduate Studies and Research

Prof. Dr. Ali Hakan Ulusoy
Acting Director

I certify that this thesis satisfies all the requirements as a thesis for the degree of Master of Science in Electrical and Electronic Engineering.

Prof. Dr. Hasan Demirel
Chair, Department of Electrical and
Electronic Engineering

We certify that we have read this thesis and that in our opinion it is fully adequate in scope and quality as a thesis for the degree of Master of Science in Electrical and Electronic Engineering.

Prof. Dr. Osman Kükreçer
Supervisor

Examining Committee

1. Prof. Dr. Hasan Kömürçügil

2. Prof. Dr. Osman Kükreçer

3. Asst. Prof. Dr. Samet Biricik

ABSTRACT

The typical two stage power inverters, a boost DC – DC converter is utilized to make a constant DC bus voltage. Then a DC – AC inverter (H- Bridge) is used to invert the DC voltage to AC voltage but in this type both of the power switches in the leg of the H – bridge cannot be turned on at the same time because it makes a short circuit and thus may damage the device. Shoot-through protection is a way used to prevent and solve this problem by controlling the shoot through state in a single phase stage quasi-switched boost inverter (qSBI). However, it has different methods, the most common is the simple boost control (SBC). This thesis presents a new pulse width modulation (PWM) control scheme to improve the modulation index for the qSBI. In this thesis, a circuit is designed with 400W and 110V and 50 HZ output. The related circuits and the operating principles were analyzed using Matlab/Simulink. The analysis simulation results proved that the control scheme can enlarge the modulation index, reduce the voltage stress on the capacitor, diode and switches, as well as reduce the frequency of the inductor current, ripples of the capacitor voltage, lowering the shoot through current.

Keywords: Pulse-Width Modulation (PWM), quasi-Z-Source Inverter (qZSI), quasi-Switched-Boost Inverter (qSBI), shoot-through, Simple Boost Control (SBC).

ÖZ

İki katmanlı güç evirgeçlerinde DA giriş gerilimi genellikle yükseltici bir DA-DA çevirgeçle elde edilir. Bunun ardından, H-köprüden oluşan bir DA-AA evirgeç kullanılarak DA gerilim AA gerilime dönüştürülür. Fakat bu tür sistemlerde, H-köprünün bir bacağındaki güç anahtarları, kısa devreye yol açıp anahtarlara zarar verebileceği için, aynı anda kapatılamazlar. Bu tür kısa devre vuruşlarına karşı koruma, tek faz yarı-anahtarlamalı yükseltici çevirgeçlerde (qSBI) kısa devre oluşumunu denetim altına alarak gerçekleştirilir. Basit yükseltici denetimi yönteminin en yaygın olduğu bu tür korumanın bir çok çeşidi vardır.

Bu tez, son zamanlarda yayınlanmış ve yarı-anahtarlamalı yükseltici çevirgeçlerde kipleme endeksini iyileştiren yeni bir darbe genişliği kipleme denetim yöntemini içeren yeni bir çalışmayı ele almaktadır. Bu çalışmada, 400 W çıkış gücü, 50 Hz 110 V çıkış gerilimine sahip bir devre çözümlenip benzetimleri yapılmıştır. İlgili devrelerin çalışma ilkeleri de Matlab/Simulink kullanılarak incelenmiştir.

Bu çözümlenme ve benzetim sonuçları, yeni yöntemin kipleme endeksini genişlettiğini, sığa, diyot ve anahtarlar üzerindeki gerilim baskısını azalttığını, bobbin akımının sıklığını azalttığını, ve kısa devre akımını da düşürdüğünü göstermiştir.

Anahtar kelimeler: Darbe Genişliği Kipleme, Yarı-Z-Kaynak- Çevirgeç, Yarı-anahtarlamalı Yükseltici Çevirgeç, Kısa Devre Vuruşu, Basit Yükseltme Denetimi.

ACKNOWLEDGMENT

First, I would like to acknowledge my supervisor, Prof. Dr. OSMAN KÜKRER for his support, guidance and encouragement throughout my work. I certainly appreciate his ongoing valuable support. No words can describe my gratitude to the person who's like another father for me, Prof. Dr. OSMAN KÜKRER.

In this acknowledgment, it is hard to forget the invaluable support and advice from the Chairman of the Electrical and Electronic Department, Prof. Dr. Hasan Demirel and the Vice-chair, Assist. Prof. Dr. Rasime Uyguroglu

I would like also to extend special thanks to my dear friend, Dr. Hamza Makhamreh for his support and invaluable assistance.

Last but not least, I would like to express my deep gratitude to my father, mother, and brother, sisters who provided me with the needed moral and financial support.

TABLE OF CONTENTS

| | |
|---|------|
| ABSTRACT..... | iii |
| ÖZ..... | iv |
| ACKNOWLEDGMENT..... | v |
| LIST OF TABLES..... | ix |
| LIST OF FIGURES..... | x |
| LIST OF SYMBOLS..... | xiii |
| LIST OF ABBREVIATIONS..... | xv |
| 1 INTRODUCTION..... | 1 |
| 1.1 Renewable Energy..... | 1 |
| 1.2 Converters..... | 1 |
| 1.3 Inverters..... | 2 |
| 1.3.1 Single Phase Half Bridge Inverter..... | 2 |
| 1.3.2 Single Phase Inverters Full Bridge (H-bridge)..... | 3 |
| 1.4 Pulse Width Modulation (PWM)..... | 4 |
| 1.5 Shoot Through Protection..... | 5 |
| 2 TYPES OF INVERTER..... | 6 |
| 2.1 Voltage Source Inverter (VSI)..... | 6 |
| 2.2 Current Source Inverters (CSIs)..... | 7 |
| 2.3 Z-Source Inverter (ZSI) and Quasi Z-Source Inverter (qZSI)..... | 7 |
| 2.4 Switched Boost Inverter (SBI)..... | 9 |
| 2.5 Quasi Switched Boost Inverter (qSBI)..... | 11 |
| 3 NEW PWM CONTROL METHOD FOR QUASI SWITCH BOOST INVERTER (qSBI)..... | 12 |

| | |
|---|----|
| 3.1 New PWM Control Method | 12 |
| 3.2 qSBI Circuit Analysis for the New PWM..... | 14 |
| 3.3 PWM Control of qSBI for The New Method..... | 16 |
| 3.4 High Frequency Peak to Peak Capacitor Voltage and Inductor Current of the New PWM Control Method | 18 |
| 3.5 Circuit and Ac Component Circuit Analysis Method for qSBI under New PWM Control Methods | 21 |
| 3.6 Limitations of Capacitance and Inductance in the New PWM Method..... | 24 |
| 4 SIMPLE BOOST CONTROL (SBC) FOR QUASI SWITCH BOOST INVERTER (qSBI)..... | 26 |
| 4.1 PWM Simple Boost Control Method for qSBI..... | 26 |
| 4.2 qSBI Circuit Analysis for SBC Method..... | 27 |
| 4.3 PWM Control of qSBI for SBC | 28 |
| 4.4 High Frequency Peak to Peak Capacitor Voltage and Inductor Current under SBC Control Method | 29 |
| 4.5 AC Component Circuit Analysis for Simple Boost Control (SBC)..... | 30 |
| 5 COMPARISON BETWEEN THE SBC METHOD AND THE NEW PWM CONTROL METHOD..... | 32 |
| 5.1 The Relation between The Boost Factor in the SBC and New PWM Methods | 32 |
| 5.2 The Relation between The Modulation Index in the SBC and New PWM Methods..... | 33 |
| 5.3 The Relation between The Duty Cycle in the SBC and New PWM Methods. | 34 |
| 5.4 Comparing the High Frequency Peak to Peak Capacitor Voltage and Inductor Current of the Conventional SBC Method and the New Method | 34 |

| | |
|--|----|
| 5.5 Governing the Equations of the SBC and the New PWM Methods | 37 |
| 5.6 Theoretical Results..... | 38 |
| 6 SIMULATION AND RESULT FOR THE NEW PWM AND SBC METHODS . | 40 |
| 6.1 Introduction | 40 |
| 6.2 Control Method Simulink Model | 42 |
| 6.2 Simulation Result | 46 |
| 6.2.1 Simulation Result of New PWM Method | 46 |
| 6.2.1.1 Simulink Result of the New PWM Method State 1 | 46 |
| 6.2.1.2 Simulink Result of The New PWM Method state 2 | 55 |
| 6.2.2 Simulation Result of SBC Method..... | 58 |
| 6.3 Comparison between the New PWM and the Conventional SBC Methods by Simulink Result..... | 64 |
| 7 CONCLUSION AND FUTURE WORK..... | 65 |
| 7.1 Conclusion | 65 |
| 7.2 Future Work | 65 |
| REFERENCES..... | 66 |

LIST OF TABLES

| | |
|---|----|
| Table 1: Comparison Between the Covering Equations of the SBC Method and New Method | 37 |
| Table 2: Parameters for the New PWM Method and SBC | 38 |
| Table 3: Theoretical Results for the New PWM Method | 38 |
| Table 4: Parameter Used For Simulink | 42 |

LIST OF FIGURES

| | |
|---|----|
| Figure 1: Boost Converter | 2 |
| Figure 2: Square Wave Output Voltage for Single Phase Half Bridge Inverter [1] | 3 |
| Figure 3: Square Wave Output Voltage for Single-Phase Full Bridge Inverter [2]..... | 4 |
| Figure 4: PWM Waveform [3] | 4 |
| Figure 5: Modes of Operation for Shoot through protection. (a) Start-up dc-link pre-charge). (b) Normal operation. (c) Shoot through before protection. (d) Shoot through after protection [4]..... | 5 |
| Figure 6: Voltage Source Inverter | 6 |
| Figure 7: Current Source Inverters | 7 |
| Figure 8: Z-source Inverter | 8 |
| Figure 9: quasi Z-source Inverter [6] | 8 |
| Figure 10: Pulse Width Modulation Method [7]..... | 9 |
| Figure 11: Switched Boost Inverter | 10 |
| Figure 12: Quasi Switched Boost Inverter | 11 |
| Figure 13: The New PWM Control Scheme for Quasi Switch Boost Inverter [9] | 13 |
| Figure 14: Quasi Switch Boost Inverter | 14 |
| Figure 15: Three Moods New PWM Control Method for qSBI [9] | 14 |
| Figure 16: Non-Shoot through State | 17 |
| Figure 17: High frequency (HF) Peak to Peak Inductor Current for New PWM Method [8] | 18 |
| Figure 18: High Frequency (HF) Peak to Peak Capacitor Voltage for the New PWM Method [8]..... | 20 |
| Figure 19: Simple Boost Control for Quasi Switch Boost Inverter [9] | 26 |

| | |
|--|----|
| Figure 20: The Operating States of Simple Boots Converter for qSBI [10] | 27 |
| Figure 21: High Frequency (HF) Peak to Peak Inductor Current and Capacitor Voltage for SBC Method [9] | 29 |
| Figure 22: Boost Factor Comparison between the Two Methods..... | 32 |
| Figure 23: Voltage Gain Comparison between the Two Methods..... | 33 |
| Figure 24: HF Peak to Peak Capacitor Voltage Comparison between the Two Methods | 35 |
| Figure 25: HF Peak to Peak Inductor Current Comparison between the Two Methods | 36 |
| Figure 26 : The Topology of the New PWM and SBC Methods..... | 41 |
| Figure 27: The Model Control of the SBC Method | 44 |
| Figure 28: The Model Control of the New PWM Method..... | 45 |
| Figure 29: Output Voltage of the New PWM Method State 1..... | 46 |
| Figure 30: Capacitor Voltage of the New PWM Method State 1 | 47 |
| Figure 31: Vdc Link Voltage of the New PWM Method State 1..... | 47 |
| Figure 32: HF Inductor Current of the New PWM Method State 1..... | 48 |
| Figure 33: HF Capacitor Voltage of the New PWM Method State 1 | 48 |
| Figure 34: Average Inductor Current of the New PWM Method State 1 | 49 |
| Figure 35: LF inductor current of the New PWM Method State 1 | 49 |
| Figure 36: LF Capacitor Voltage of the New PWM Method State 1..... | 50 |
| Figure 37: Vds Voltage of Switch 5 of the New PWM Method State 1 | 50 |
| Figure 38: Vds Voltage of Switch 1 of the New PWM Method State 1 | 51 |
| Figure 39: Output Current of the New PWM Method State 1 | 51 |
| Figure 40: THD Output Current of the New PWM Method State 1 | 52 |
| Figure 41: Output Voltage of Load Changing for the New PWM Method State 1 ... | 53 |

Figure 42: Output Current of Load Changing for the New PWM Method State 1 53

Figure 43: Capacitor Voltage of Load Changing for the New PWM Method State 154

Figure 44: Inductor Current of Load Change for the New PWM Method State 1 54

Figure 45: Output Voltage New PWM Method State 2..... 55

Figure 46: Capacitor Voltage of the New PWM Method State 2 55

Figure 47: Average Inductor Current of the New PWM Method State 2 56

Figure 48: HF Inductor Current of the New PWM Method State 2..... 56

Figure 49: HF Capacitor Voltage of the New PWM Method State 2 57

Figure 50: THD Output Current of the New PWM Method State 2..... 57

Figure 51: Output Voltage for SBC Method..... 58

Figure 52: Capacitor Voltage for SBC Method 58

Figure 53: Dc Link Voltage for SBC Method..... 59

Figure 54: HF Inductor Ripple Current for SBC Method 59

Figure 55: HF capacitor voltage for SBC Method 60

Figure 56: Inductor Current for SBC Method..... 60

Figure 57: Low frequency Inductor Current for SBC Method 61

Figure 58: Low Frequency of Capacitor Voltage for SBC Method..... 61

Figure 59: Switch 5 Voltage for SBC Method..... 62

Figure 60: Switch 1 voltage for SBC Method..... 62

Figure 61: Output Current for SBC Method 63

Figure 62: THD Output Current for SBC Method 63

LIST OF SYMBOLS

| | |
|--------------|--|
| B_S | The Boost Factor in SBC |
| B_P | The Boost Factor for the New Method |
| V_C | Capacitor Voltage |
| V_{PN} | DC-link Voltage |
| I_{PN} | DC-link Current |
| G_S | Voltage Gain for SBC |
| G_P | Voltage Gain for the New Method |
| ΔI_L | High Frequency Peak-to-Peak Inductor Ripple Current |
| ΔV_C | High Frequency Peak-to-Peak Capacitor Ripple Voltage |
| \hat{i}_L | Peak Value of Low Frequency Inductor Current |
| \hat{v}_C | Peak Value of Low Frequency Capacitor Voltage |
| I_{PN} | Non-Shoot-through dc-link Current |
| D_0 | Shoot-Through Duty Ratio for the new method |
| D | Shoot-Through Duty Ratio for the SBC |
| P_o | Rated Power |
| V_{dc} | Input Voltage Range |
| V_o | Output Voltage |
| D_a, D_b | Diodes |
| S | Switching |
| M | Modulation Index |

| | |
|-----------|--------------------------------|
| L | Inductor |
| C | Capacitor |
| I_L | Maximum Input Current |
| T | Time Period |
| φ | Impedance Angle |
| ω | Angular Frequency |
| I_m | Amplitude of Current |
| V_m | Amplitude of AC Output Voltage |

LIST OF ABBREVIATIONS

| | |
|------|-------------------------------|
| HF | High Frequency |
| LF | Low Frequency |
| PWM | Pulse Width Modulation |
| qSBI | Quasi Switched Boost Inverter |
| qZSI | Quasi Z-Source Inverter |
| RMS | Root Mean Square Value |
| SBC | Simple Boost Inverter |
| SBI | Switched Boost Inverter |
| THD | Total Harmonic Distortion |
| ZSI | Z-Source Inverter |

Chapter 1

INTRODUCTION

1.1 Renewable Energy

The demand of energy is increasing day by day because of the rapid rise in population and developments. Due to the rapid depletion of fossil fuel these non-renewable sources cannot meet the required demand. This is in addition to the bad effects on environment due to the emission of CO_2 during combustion. Renewable energy system based on solar-wind energy could be considered as a useful solution. It serves as a bridge which portrays typical renewable distributed power generation system using photovoltaic and wind as energy source.

These renewable energy systems need power conversion through converters and inverters to interface between their load and source. The output voltage in solar photovoltaic and fuel cell is low and has to be high voltage ac output, in addition to boost dc-dc converter, so the power conversion will be with two-stage dc-dc-ac.

1.2 Converters

DC-to-DC converter (chopper) is a device that converts from input DC voltage to the required output DC voltage. Converters can boost converters (transform to higher voltage level), buck converters (convert from a voltage level to a relatively lower voltage level), or buck-boost converters (converter which can either be a buck or a boost converter based on its control signals).

The high step-up (Boost Converter) converts from low level voltage to high level voltage and it needs the components: diode, inductor electronic switch (MOSFET) and output capacitor as shown in Figure 1.

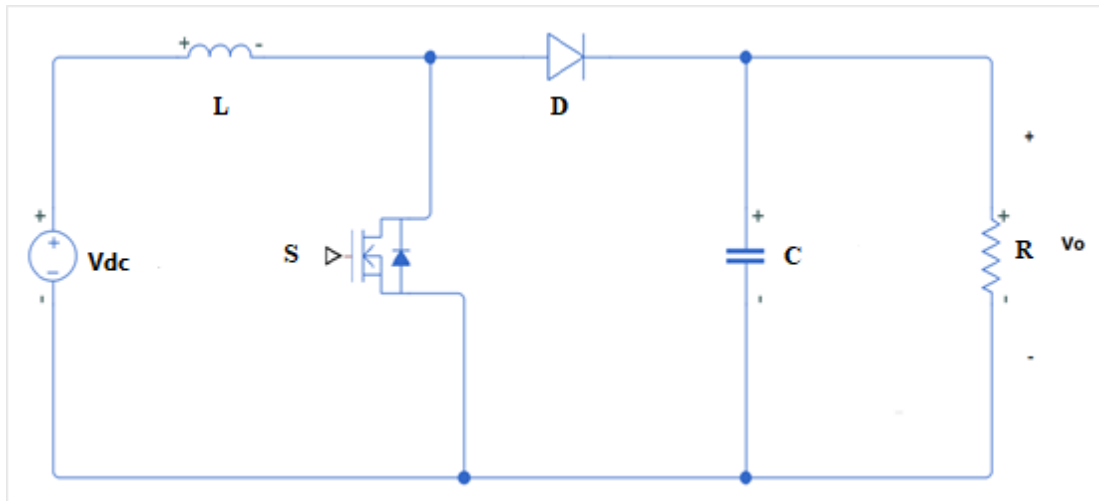


Figure 1: Boost Converter

1.3 Inverters

Power inverter is an electronic device that converts DC power to standard AC power which means that the current and voltage have variable values with respect to time. Single phase inverters have many types depending on the application purpose. There are two main types of inverters, the single-phase half bridge and single-phase full bridge (H-bridge) inverters. These inverters can be categorized according to the main types that will discuss later.

1.3.1 Single Phase Half Bridge Inverter

Single phase half Bridge inverter has two electronic switches, and it can use the insulated gate bipolar transistor (IGBT) antiparallel diodes or (MOSFET). The freewheeling diodes is connected to pass the negative current produced from the inductive load. The two switches cannot be turned on at the same time as it may cause a short circuit called shoot through the DC link divided into two capacitors with equal

voltage. When S_1 is turned on, it will produce output voltage equal to $V_{dc} / 2$. On the other hand, the other switch will turn off and the output voltage will be $-V_{dc} / 2$, this will produce a square wave output voltage as shown in Figure 2.

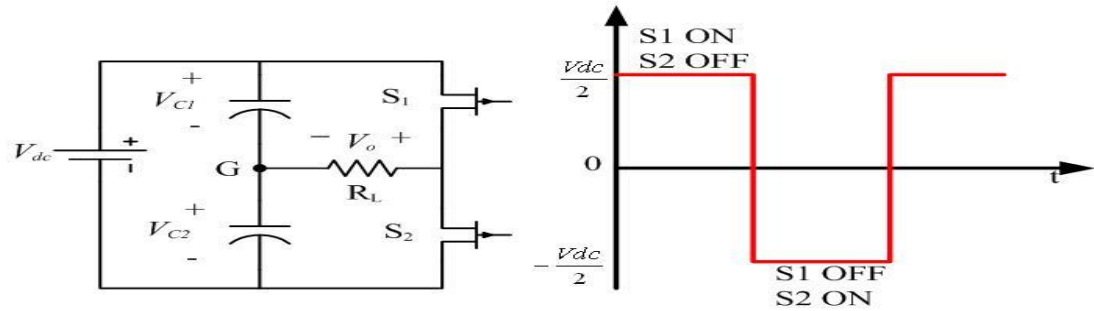


Figure 2: Square Wave Output Voltage for Single Phase Half Bridge Inverter [1]

1.3.2 Single Phase Inverters Full Bridge (H-bridge)

This H-bridge inverter consists of two half-bridge legs and four electronic switches (semiconductor devices). The freewheeling diodes is connected to pass the negative current produced from the inductive load. When $S_1 - S_4$ ON and $S_3 - S_2$ are OFF then V_{a0} equals $V_s / 2$ and V_{b0} equals $-V_s / 2$ so the output will be V_s . On the other hand, when $S_3 - S_2$ are ON and $S_1 - S_4$ are OFF V_{a0} equals $-V_s / 2$ and V_{b0} equals $V_s / 2$ and the output will be $-V_s$, as shown in Figure 3.

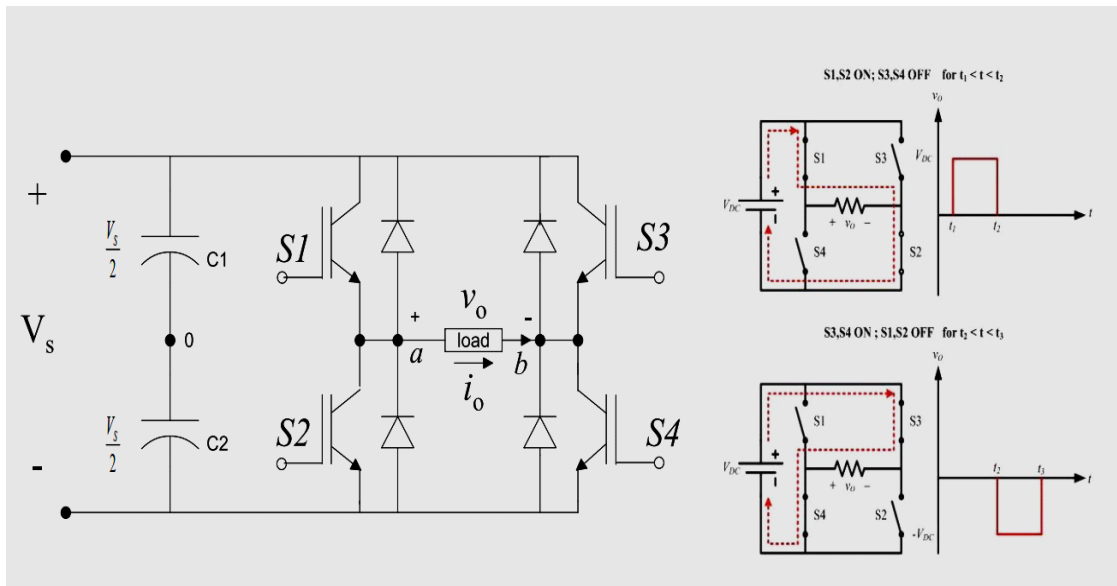


Figure 3: Square Wave Output Voltage for Single-Phase Full Bridge Inverter [2]

1.4 Pulse Width Modulation (PWM)

A technique used to control the power electronic switches such as transistors. This technique has different pulse width durations (δ) and same amplitude. The pulse width modulation is used for control as it causes less total harmonic distortion than square wave. It uses operator to generate triangular wave (carrier) and sine wave (modulating) then it compares them to obtain the PWM wave form as shown in Figure 4.

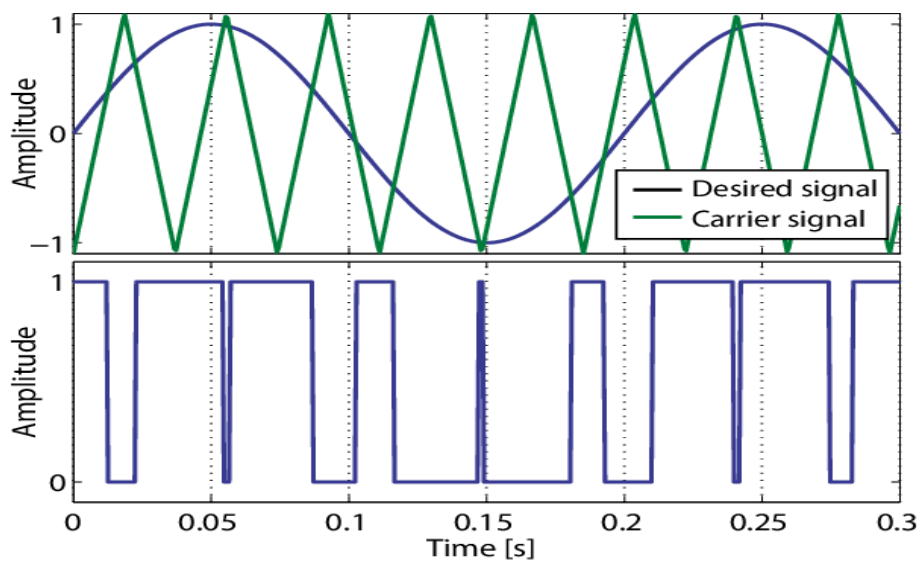


Figure 4: PWM Waveform [3]

1.5 Shoot Through Protection

Shoot through protection is used for shorting the inverter dc bus and it occurs in a leg of H-bridge inverter when the two semiconductor switches are turned ON at the same time. The short-circuit current can rapidly rise to higher than the current limit of the semiconductor devices and it occurs in few microseconds. This will cause the semiconductor to destroy.

To solve the shoot through problem, a shoot-through protection scheme is used, and it consists of bidirectional switch, compounded by a Si insulated-gate bipolar transistor (IGBT) and a relay. It is embedded into the dc-link midpoint in order to detect and clear shoot-through faults. The Figure 5 describes how it works [4].

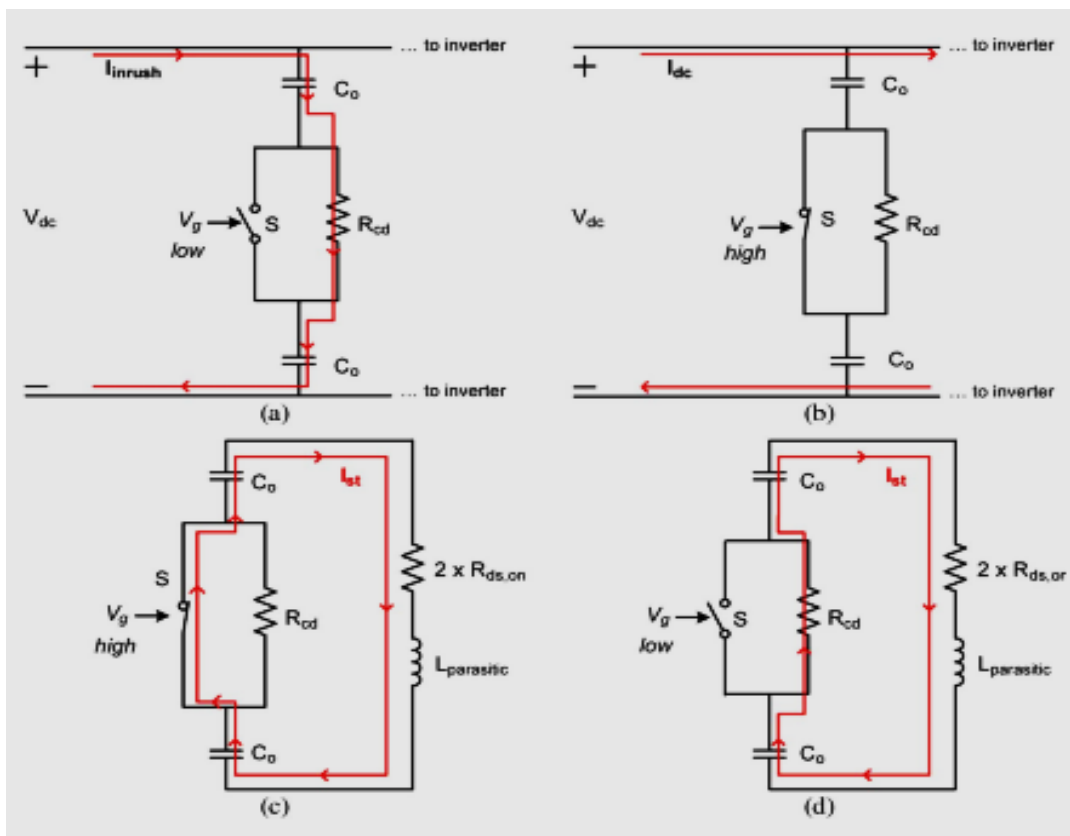


Figure 5: Modes of Operation for Shoot through protection. (a) Start-up dc-link pre-charge). (b) Normal operation. (c) Shoot through before protection. (d) Shoot through after protection [4]

Chapter 2

TYPES OF INVERTER

2.1 Voltage Source Inverter (VSI)

Usually VSIs are connected with fixed voltage photovoltaic source or battery, therefore it is used in application where low and medium power is needed. The capacitor connected to the inverter is large and can be considered as an ideal voltage source, and the input of the inverter cannot be short circuited.

VSIs shown in Figure 6 suffer from that, it must have an input voltage which is greater than the peak value of the output voltage. This limits the high voltage operation of VSI motor controllers and the low voltage and hence results in low speed.

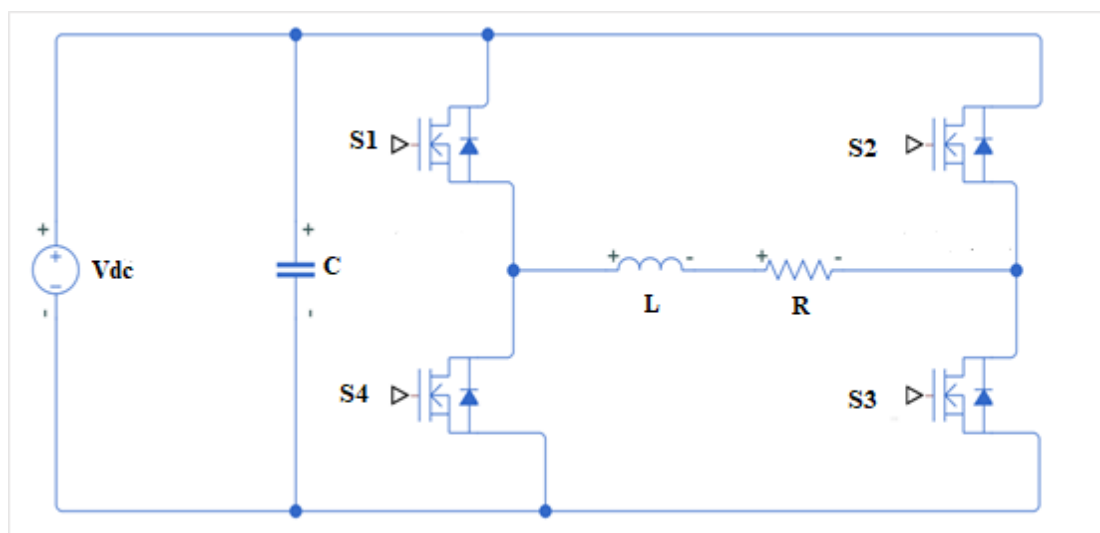


Figure 6: Voltage Source Inverter

2.2 Current Source Inverters (CSIs)

CSI is used for medium voltage and high-power loads. The inductor is large and can be considered as an ideal current source. The input of the inverter cannot be open circuited, as shown in Figure 7.

CSI must have an input voltage which is less than the peak value of the output voltage.

Since the source in a practical CSI cannot maintain bidirectional power flow.

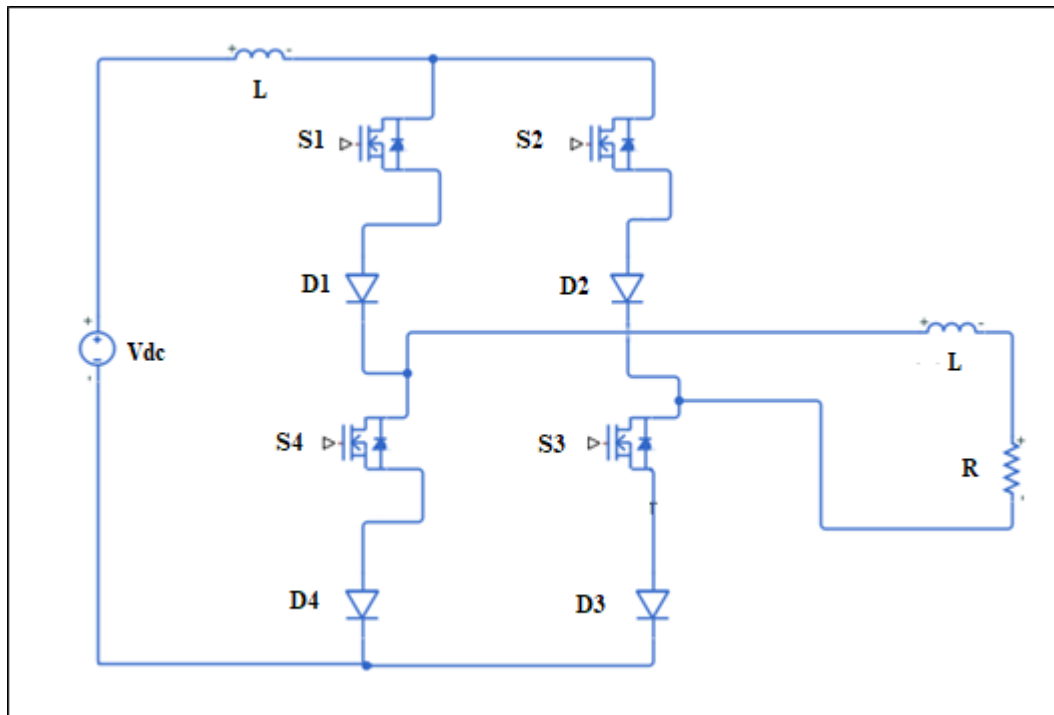


Figure 7: Current Source Inverters

2.3 Z-Source Inverter (ZSI) and Quasi Z-Source Inverter (qZSI)

Z-source inverter consists of impedance to couple the converter main circuit to the power source. This impedance consists of two inductors and two capacitors as shown in Figure 8. ZSI provides advantages that cannot be obtained in the traditional voltage-source and current-source converters which overcomes both the output voltage limitation and the shoot-through problem with single-stage power conversion. It is

used to improve the input current profile and to reduce the voltage stress on the capacitor. The Z-source concept can be applied to all ac-to-dc, ac-to-dc dc-to-ac, dc-to-dc and ac-to-ac power conversions [5].

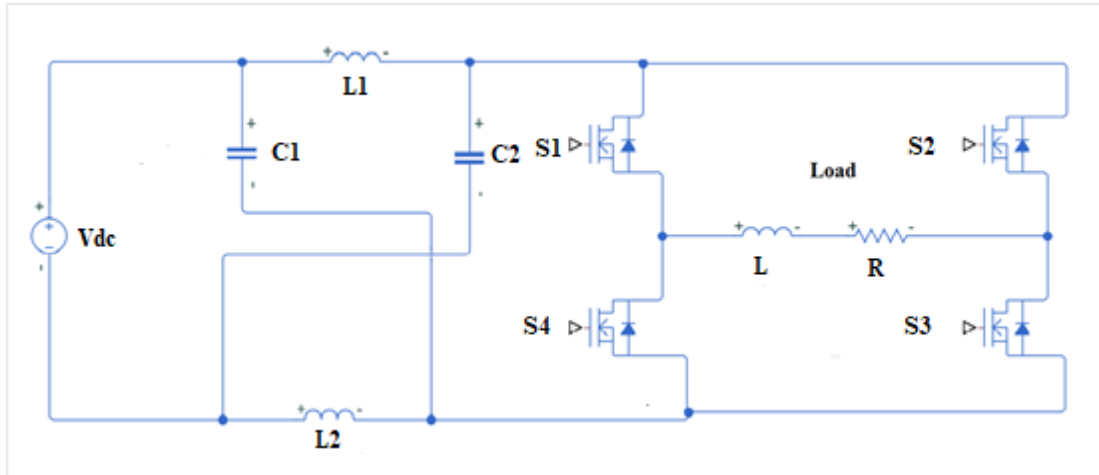


Figure 8: Z-source Inverter

The voltage fed ZSI has some disadvantages. The input current is discontinuous in the boost mode and the capacitors must sustain a high voltage. The inductors must sustain high currents in ZSI to developed ZSI to overcome this issue by using qZSI as shown in Figure 9. qZSI has lower dc voltage on Capacitors C1 and C2 and Lower current in inductors L1 and L2.

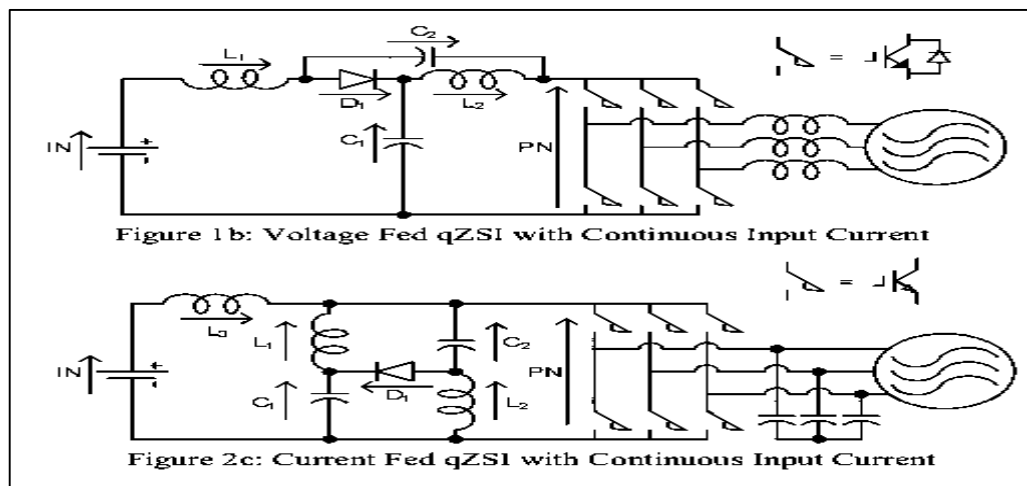


Figure 9: quasi Z-source Inverter [6]

ZSI inverter uses the shoot through states to boost the dc bus voltage and produce a desired output voltage that is greater than the available dc bus voltage by gating on both upper and lower switches of a phase leg. Maximum boost control (MBC) method use the relationship between the modulation index and the voltage boost to achieve maximum voltage boost and to improve the voltage gain by using PWM as shown in Figure 10. Maximum constant boost control (MCBC) method, which can obtain maximum voltage gain at any given modulation index without producing any low-frequency ripple that is related to the output frequency and minimize the voltage stress at the same time [5].

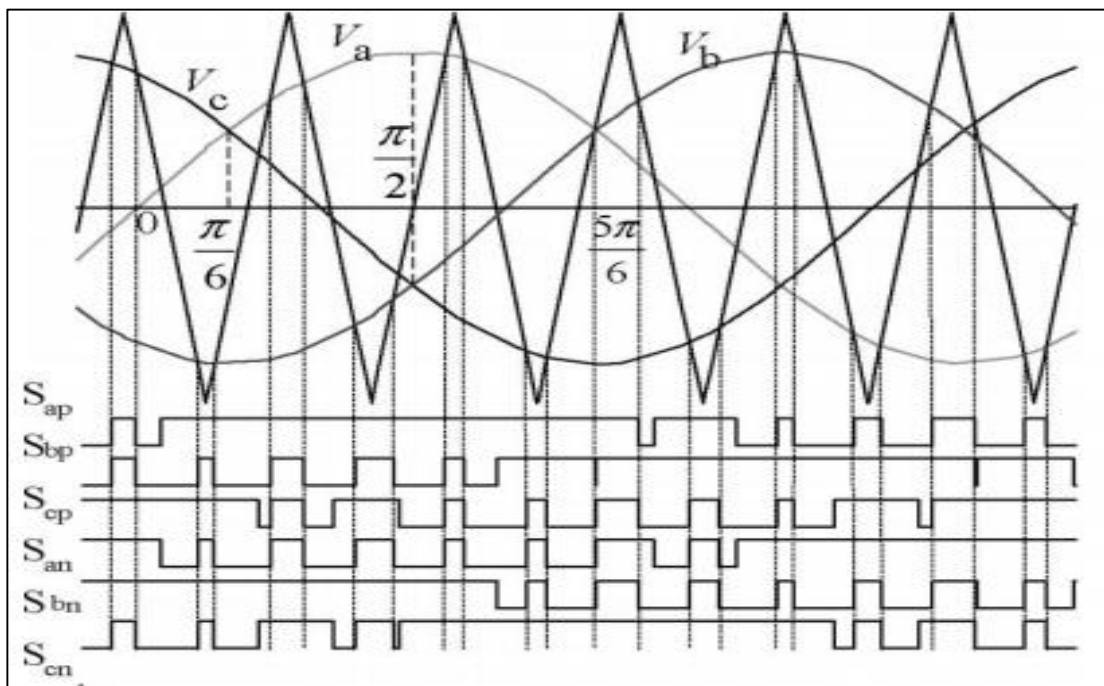


Figure 10: Pulse Width Modulation Method [7]

2.4 Switched Boost Inverter (SBI)

The switched boost inverter SBI is a single or one stage power converter which converts dc voltage into ac voltage and supplies both ac and dc loads simultaneously from a single dc input (dc input is obtained from the solar panel). SBI can produce an

ac output voltage, which is either greater or less than the available dc input and thereby has an advantage of wide range of obtainable output voltage for a given dc input voltage. SBI can be used instead of a Z-source inverter (ZSI) in low-power applications since the ZSI increases the size and cost of the power inverter. The weight, size, and cost are main considerations in this inverter. The SBI has the same advantages as the ZSI in the shoot-through operation which is capable of voltage boosting and inversion is required. The main components are an electronic switch (S), inductor (L), capacitor (C), high speed diode (D), and DC voltage source (V_{dc}) as shown in Figure 11. The gain in SBI is less than ZSI due to the current-fed switched inverter (CFSI) used to improve the boost factor and the input current profile, which has the two features it combines the high-gain of ZSI and a few passive component of SBI. The capacitor voltage stress in SBI is equal to the dc-link voltage, which has a high voltage stress on the capacitor when a high boost is used and the current drawn from the source is discontinuous because it directly connects to the diode.

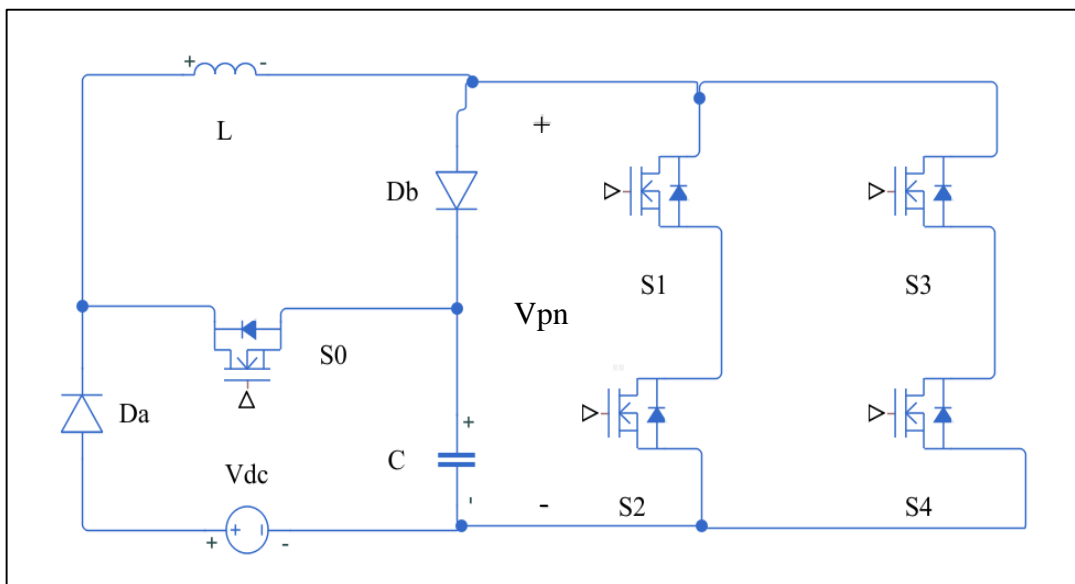


Figure 11: Switched Boost Inverter

2.5 Quasi Switched Boost Inverter (qSBI)

Quasi switched boost inverter (qSBI) uses one less capacitor with low capacitance and one less inductor with higher inductance but its use one more active switch and one more diode than Z-source Inverter (qZSI). Figure 12 shows the single-phase qSBI topology it includes one inductor (L), one capacitor (C), six diodes, five active switches, and a passive load (R and L_1). (qSBI) have several advantages over qZSI, it has lower current rating on its switches and diodes also it has higher boost factor with an equivalent parasitic effect and finally higher efficiency. Moreover, qZSI have several advantages compared with a conventional SBI it is reduce the voltage stress on the capacitor, increase the boost voltage factor, and improve the input current profiles. the shoot-through occur in power switches leg when turned on at the same time it used to step up the voltage but when it uses a large shoot through to boost the voltage the modulation index will be low this will causes increasing the total harmonic distortion(THD) and decreasing the dc-ac inversion. qSBI will be discuss in detail in chapter 3 and 4.

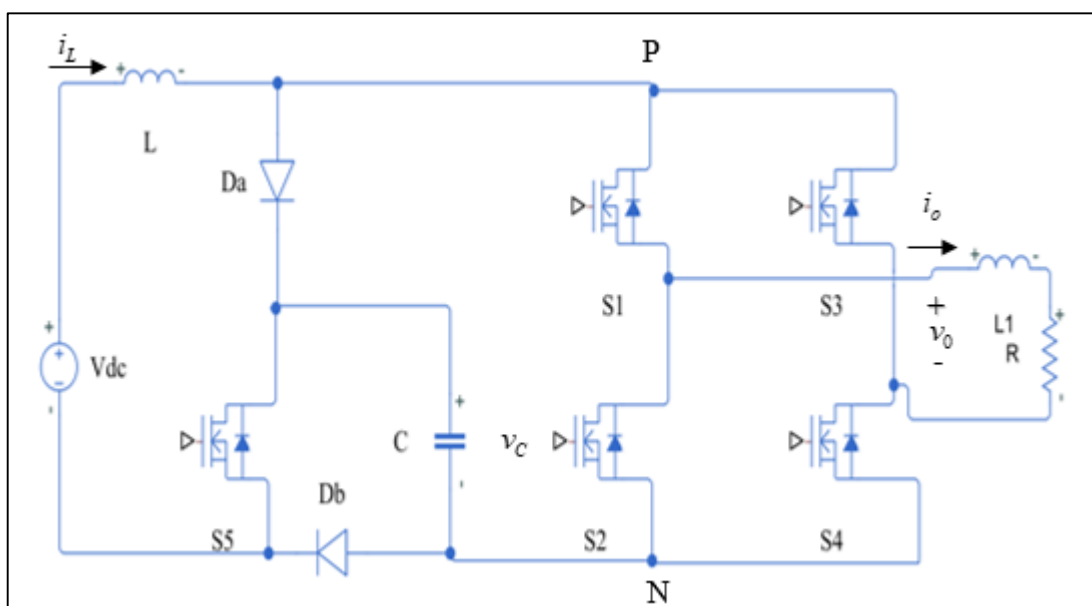


Figure 12: Quasi Switched Boost Inverter

Chapter 3

NEW PWM CONTROL METHOD FOR QUASI SWITCH BOOST INVERTER (qSBI)

3.1 New PWM Control Method

A new PWM control method applied on a single-phase single stage (qSBI) has more advantages than control method for qSBI [9]. The new PWM method uses higher modulation index to produce same voltage gain as SBC. This will result in reducing the voltage stress on the capacitor, diodes and switches under this new PWM control method. This control method has one more operating state when switch S_5 is turned on during non-shoot-through state of the H-bridge of qSBI. This chapter will address this control in details and compare between the new PWM control method and simple boost converter for single phase qSBI.

The new PWM control scheme shown in Figure 13 a high frequency (HF) saw tooth waveform v_{saw} with amplitude 2 is compared with a constant voltage V_{SH} to generate a control signal for S_5 . Moreover, HF wave triangle v_{tri1} with amplitude 1 is compared to V_{SH} for generating the shoot through control signal. The two control waveforms v_{con} and $-v_{con}$ are compared with the high frequency triangle (dashed line) waveform v_{tri2} to generate control signal for switches (S_1 - S_4). Then the shoot through signal is inserted into the control signal of switches (S_1 - S_4) through other logic gates to generate

shoot through state. The value of V_{SH} is determined as $(1-D)$ and is defined by the shoot through duty cycle.

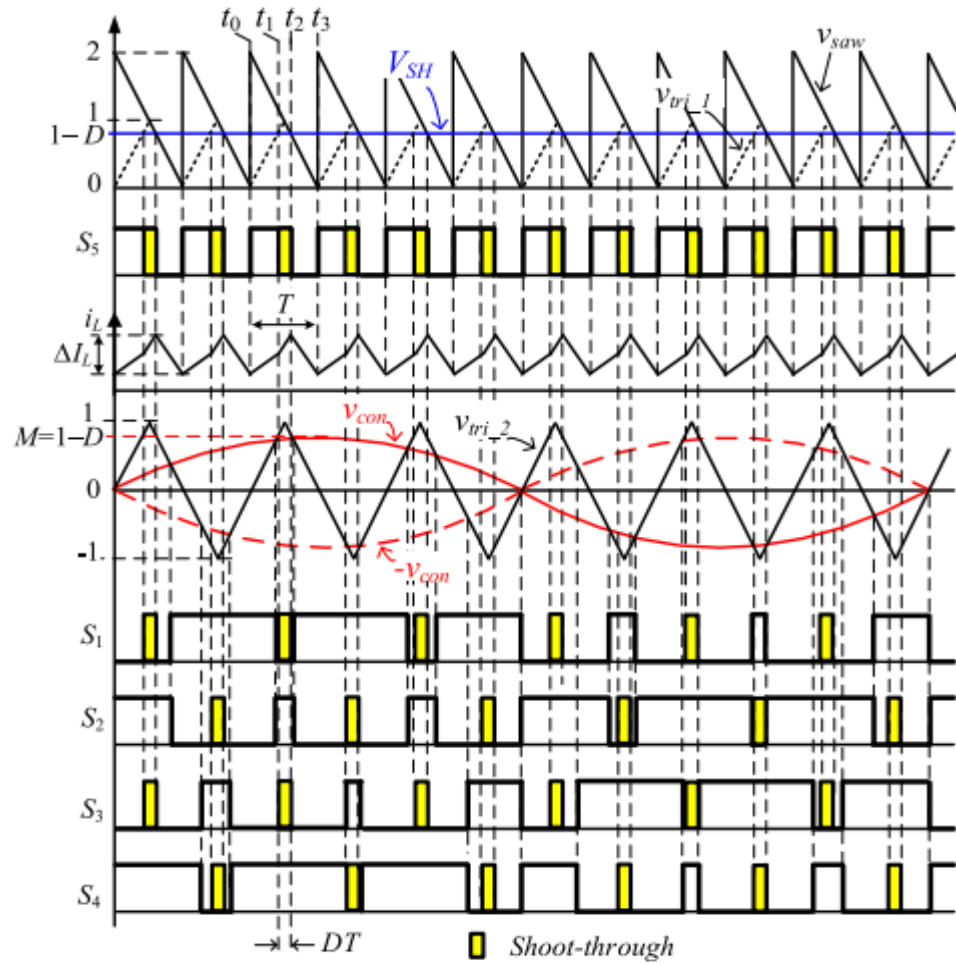


Figure 13: The New PWM Control Scheme for Quasi Switch Boost Inverter [9]

3.2 qSBI Circuit Analysis for the New PWM

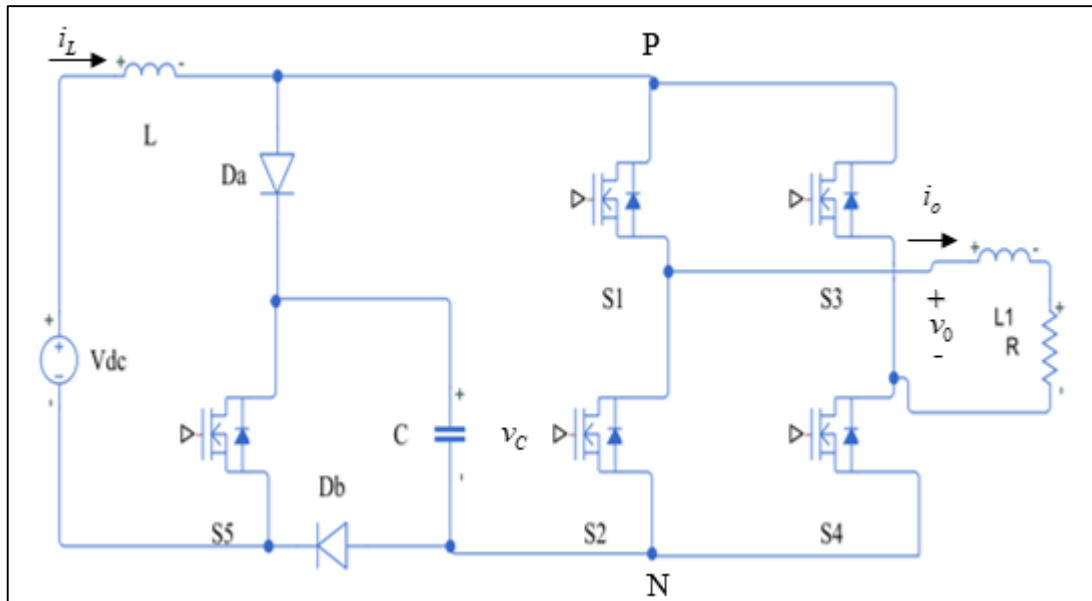


Figure 14: Quasi Switch Boost Inverter

qSBI operating in 3 moods for three different time intervals as shown in Figure 15

1. Shoot through $[t_1, t_2]$
2. Non-shoot through 1 $[t_2, t_3]$
3. Non-shoot through 2 $[t_0, t_2]$

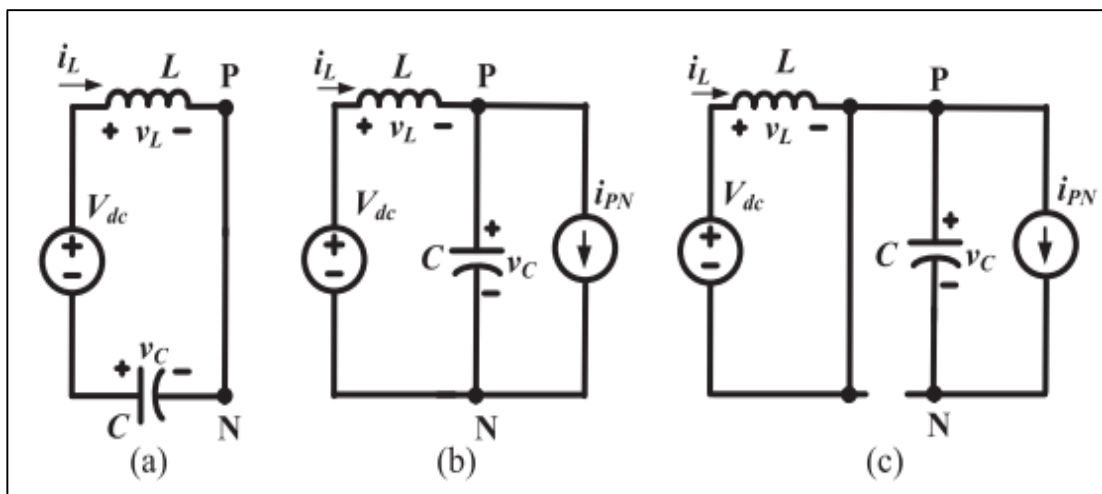


Figure 15: Three Moods New PWM Control Method for qSBI [9]

The first state Figure 15 (a) is shoot through $[t_1, t_2]$, in this state all the power switches for qSBI are turned on. The time interval of this state is DT , D is the duty ratio and T is the switching period in this state.

$$\begin{cases} L \frac{di_L}{dt} = V_{dc} + V_C \\ C \frac{dV_C}{dt} = -I_L \end{cases} \quad (1)$$

The second state Figure 15 (b) is non-shoot through $[t_2, t_3]$. In this state, switch S_5 is turned off as shown in Fig, the H-bridge operates in zero state and active state. The time interval is $(1-D) T/2$.

$$\begin{cases} L \frac{di_L}{dt} = V_{dc} - V_C \\ C \frac{dV_C}{dt} = I_L - I_{PN} \end{cases} \quad (2)$$

The third state Figure 15 (C) is non-shoot through $[t_0, t_1]$. In this state the switch S_5 is turned on as shown in the Fig, H- bridge work in zero and active state and the time interval in this state $(1-D) T/2$.

$$\begin{cases} L \frac{di_L}{dt} = V_{dc} \\ C \frac{dV_C}{dt} = -I_{PN} \end{cases} \quad (3)$$

From the second balance principle equation for the capacitor and math simplification we get

$$\begin{aligned} (V_{dc} + V_C)DT + (V_{dc} - V_C) \frac{1-D}{2} + V_{dc} \frac{1-D}{2} &= 0 \\ \Rightarrow V_{dc} \left[D + \frac{1-D}{2} + \frac{1-D}{2} \right] + V_C \left[D - \left(\frac{1-D}{2} \right) \right] &= 0 \\ \Rightarrow V_{dc} + V_C \left[\frac{3}{2}D - \frac{1}{2} \right] &= 0 \end{aligned}$$

$$V_C = \frac{2}{1-3D} V_{dc} \quad (4)$$

From the second balance principle equation for the inductor we get

$$-I_L D + (I_L - I_{PN}) \frac{1-D}{2} - I_{PN} \frac{1-D}{2} = 0$$

$$\Rightarrow I_L \left[-D + \frac{1-D}{2} \right] - I_{PN} (1-D) = 0$$

$$\Rightarrow I_{PN} = \frac{\left(\frac{1}{2} - \frac{3}{2} D \right)}{1-D} I_L$$

$$I_{PN} = \frac{1-3D}{2(1-D)} I_L \quad (5)$$

The peak dc link voltage in the non-shoot through states is calculated by

$$V_{PN} = V_C = \frac{2}{1-3D} V_{dc} \quad (6)$$

3.3 PWM Control of qSBI for The New Method

Under the new PWM control method shows a high boost invention ability and this high boost ratio dramatically increases the inverter switch voltage stress. The boost factor in qSBI under new PWM control is expressed by

$$B_p = \frac{V_{PN}}{V_{dc}} = \frac{2}{1-3D} \quad (7)$$

The dc-ac inversion voltage gain is expressed as

$$G = \frac{\hat{v}_0}{V_{dc}} = M.B \quad (8)$$

Where B is the boost factor and \hat{v}_0 is the peak value of the output voltage. A high quality of output voltage and the amplitude value of v_{con} is not set higher than V_{SH} also the maximum duty cycle of the shoot-through state is $(1-M)$. The voltage gain (MB) for the new PWM control method is defined by G_p .

$$G_p = M.B_p = \frac{2M}{3M-2} \quad (9)$$

If qSBI is forced to operate in non-shoot mode only the diode D_a is forward biased and this will result in the qSBI which becomes two stage inverter with the boost dc-dc converter of $C-D_b-S_5-L$ and the dc-link voltage (V_{PN}) equal to output voltage of the boost converter. By assuming the first state, non-shoot through $[t_a - t_b]$ and the second state non-shoot through $[t_b - t_c]$ as seen in Figure 16

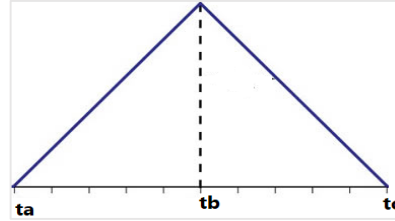


Figure 16: Non-Shoot through State

For the first state:

$$L \frac{di}{dt} = V_{dc} - V_C$$

For the second state

$$L \frac{di}{dt} = V_{dc}$$

Applying the volt second principle in steady state

$$(V_{dc} - V_C)(1 - D') + V_{dc}(D') = 0$$

$$\Rightarrow V_{dc}[1 - D' + D'] = V_C(1 - D)$$

$$\Rightarrow V_C = \frac{1}{1 - D'} V_{dc} \quad \text{Note that } V_C = V_{PN}$$

$$B_p = \frac{V_{PN}}{V_{dc}} = \frac{1}{1-D_B} \quad (10)$$

Where D_b is the duty cycle of the switch S_5 .

Duty cycle range for switch S_5 from 0 to 1 in this case, the converter is forced to operate in non-shoot through state only .and when the shoot through duty cycle is zero so $D_b = 0.5$ and the boost factor is equal to 2.

3.4 High Frequency Peak to Peak Capacitor Voltage and Inductor Current of the New PWM Control Method

Figure 17 shows the high frequency peak to peak inductor current divided into three states.

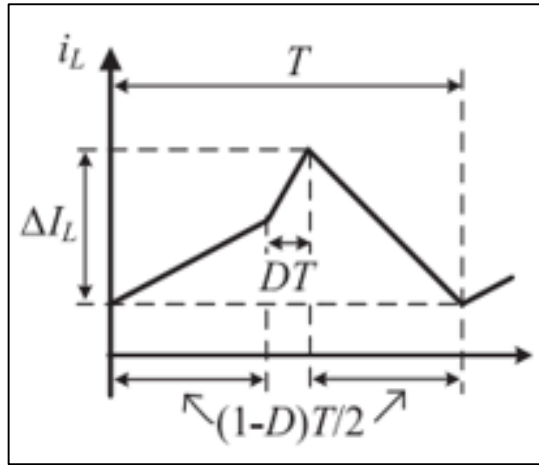


Figure 17: High frequency (HF) Peak to Peak Inductor Current for New PWM Method [8]

a) In non-shoot through $[t_0 - t_1]$

$$L \frac{di}{dt} = V_{dc}$$

$$\Rightarrow L \frac{\Delta I_1}{\Delta T_1} = V_{dc}$$

$$\Rightarrow \Delta I_1 = \left(\frac{1-D}{2L} \right) T_s \cdot V_{dc}$$

b) In shoot through $[t_1 - t_2]$

$$L \frac{di}{dt} = V_{dc} + V_C$$

$$\Rightarrow L \frac{\Delta I_2}{\Delta T_2} = V_{dc} + V_C$$

$$\Rightarrow \Delta I_2 = (V_{dc} + V_C) \frac{DT}{L}$$

Thus total high frequency (HF) peak to peak inductor current

$$\Delta I_L = \frac{1}{L} \left[\frac{(1-D)T}{2} V_{dc} + DT(V_{dc} + V_C) \right]$$

$$\Rightarrow \frac{T}{L} \left[\left(\frac{1}{2} - \frac{1}{2}D + D \right) V_{dc} + DV_C \right]$$

By substituting the value of V_C from equation (4)

$$\Rightarrow \frac{T}{L} \left[\left(\frac{1}{2} + \frac{1}{2}D \right) V_{dc} + \frac{2D}{1-3D} V_{dc} \right]$$

$$\Rightarrow \frac{T}{2L} V_{dc} \left[1 + D + \frac{4D}{1-3D} \right]$$

$$\Rightarrow \frac{T}{2L} V_{dc} \left[\frac{(1+D)(1-3D) + 4D}{(1-3D)} \right]$$

$$\Delta I_L = \frac{TV_{dc}(1-D)(1+3D)}{2L(1-3D)} \quad (11)$$

As seen in Figure 18, the high frequency peak to peak capacitor voltage into three states.

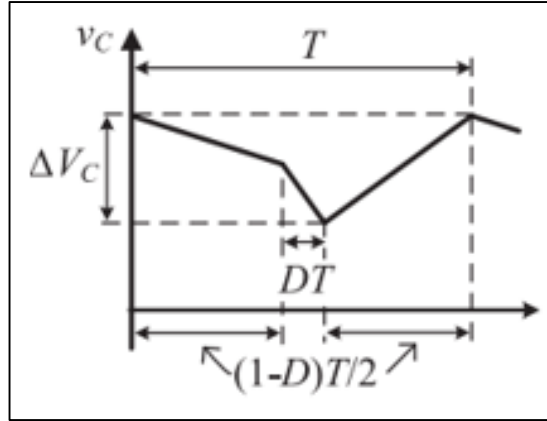


Figure 18: High Frequency (HF) Peak to Peak Capacitor Voltage for the New PWM Method [8]

a) In non-shoot through [$t_0 - t_1$]

$$C \frac{dv_C}{dt} = -I_{PN}$$

$$\Rightarrow C \frac{\Delta V_1}{\Delta T_1} = -I_{PN}$$

$$\Rightarrow \Delta V_1 = \left(\frac{1-D}{2C} \right) T_S \cdot (-I_{PN})$$

b) In shoot through [$t_1 - t_2$]

$$C \frac{dv_C}{dt} = -I_L$$

$$\Rightarrow C \frac{\Delta V_2}{\Delta T_2} = -I_L$$

$$\Rightarrow \Delta V_2 = -I_L \cdot \frac{DT}{C}$$

Thus the total high frequency (HF) peak to peak capacitor voltage

$$\Delta V_C = \frac{1}{C} \left[I_{PN} \frac{1-D}{2} T + I_L DT \right]$$

$$\Rightarrow \frac{T}{2C} [(1-D)I_{PN} + 2DI_L]$$

By substituting the value of I_{PN} from equation (5) will define as

$$\Rightarrow \frac{T}{2C} \left[(1-D) \frac{1-3D}{2(1-D)} + 2D \right] I_L$$

$$\Delta V_C = \frac{TI_L(1+D)}{4C} \quad (12)$$

3.5 Circuit and Ac Component Circuit Analysis Method for qSBI under New PWM Control Methods

The fundamental voltage of the current and the ac output of the qSBI is obtained as

$$\begin{cases} v_0 = V_m \sin \omega t \\ i_0 = I_m \sin(\omega t - \varphi) \end{cases} \quad (13)$$

It is known that the power generated by dc link in non-shoot through is equal to output power and is defined by

$$p_0 = (1-D) V_{PN} \cdot i_{PN_non} = v_o \cdot i_0$$

$$p_0 = V_m \sin \omega t \cdot I_m \sin(\omega t - \varphi) \quad (14)$$

But with the relation between the modulation index and the dc-link voltage is that

$V_m = M \cdot V_{PN}$, the dc-link current for the non-shoot through state is defined by.

$$i_{PN_non} = \frac{MI_m \cos \varphi}{2(1-D)} - \frac{MI_m \cos(2\omega t - \varphi)}{2(1-D)} \quad (15)$$

$$i_{PN_non} = I_{PN_non} + \hat{i}_{PN_non} \quad (16)$$

Where I_{PN_non} is the dc component and \hat{i}_{PN_non} is the low frequency component of the dc-link current in the non-shoot through.

If assumed that ac component circuit analysis for qSBI as follows:

1. qSBI inverter operate in a continuous conduction mode .
2. All diodes, inductors and switches are ideal and loss.

3. The small signal perturbation around the equivalent point of the variable are donated by symbol “^” above these variables.
4. The dc voltage source is constant.

It is obtained in shoot-through form the assumption mentioned above that.

In shoot through state

$$\begin{cases} L \frac{d\hat{i}}{dt} = \hat{v}_c \\ C \frac{d\hat{v}_c}{dt} = -\hat{i}_L \end{cases} \quad (17)$$

In non-shoot through (1)

$$\begin{cases} L \frac{d\hat{i}}{dt} = -\hat{v}_c \\ C \frac{d\hat{v}_c}{dt} = -\hat{i}_L - \hat{i}_{PN_non} \end{cases} \quad (18)$$

In non-shoot through (2)

$$\begin{cases} L \frac{d\hat{i}}{dt} = 0 \\ C \frac{d\hat{v}_c}{dt} = -\hat{i}_{PN_non} \end{cases} \quad (19)$$

By applying small signal analysis method, the state-space averaged model of the simplified qSBI will result as follows

$$\begin{cases} L \frac{d\hat{i}}{dt} = (D + \hat{d}) \cdot (v_c) + \left(\frac{1-D-\hat{d}}{2} \right) \cdot (-\hat{v}_c) \\ C \frac{d\hat{v}_c}{dt} = (D + \hat{d}) \cdot (-i_L) + (1-D-d) \cdot \left(\frac{1}{2} \hat{i}_L - \hat{i}_{PN_non} \right) \end{cases} \quad (20)$$

The small signal in the shoot through duty cycle (\hat{d}) can be minimized through reasonable control design and the effect of \hat{d} for LF ripples of the capacitor voltage

and inductor current is less important than that of the dc link LF current ripples \hat{i}_{PN_non} . The small signal perturbation of the shoot through should be ignored. Thus solving equation(20) with $\hat{d}=0$ the LF 2ω inductor current and capacitor voltage can be defined as

$$\begin{cases} j2\omega L\hat{i}_L = D\hat{v}_C - \frac{1}{2}(1-D)\hat{v}_C \\ j2\omega C\hat{v}_C = \left(-D + \frac{1}{2}(1-D)\right)\hat{i}_L - (1-D)\hat{i}_{PN_non} \end{cases}$$

$$\begin{cases} 2j\omega L\hat{i}_L = \left(\frac{3}{2}D - \frac{1}{2}\right)\hat{v}_C \\ 2j\omega L\hat{v}_C = \left(\frac{1-3D}{2}\right)\hat{i}_L - (1-D)\hat{i}_{PN_non} \end{cases} \quad (21)$$

By substituting \hat{v}_C into the first term in equation (21) we get

$$\begin{aligned} j2\omega L\hat{i}_L &= \frac{1}{2}(3D-1)\left(\frac{1}{j2\omega C} \frac{1}{2}(1-3D)\hat{i}_L - \frac{1-D}{j2\omega C}\hat{i}_{PN_non}\right) \\ \Rightarrow \left(j2\omega L + \frac{(1-3D)^2}{j8\omega C}\right)\hat{i}_L &= \left(\frac{(1-3D)(1-D)}{j4\omega C}\right)\hat{i}_{PN_non} \\ \Rightarrow \hat{i}_L &= \frac{-2(1-3D)(1-D)}{16\omega^2 LC(1-D)^2}\hat{i}_{PN_non} \end{aligned}$$

By substituting the low frequency component of the dc-link current \hat{i}_{PN_non} from equation (15) the LF inductor current can be calculated as

$$\hat{i}_L = \frac{(1-3D)MI_M}{16\omega^2 LC - (1-3D)^2} \quad (22)$$

Put \hat{i}_L in equation (21) the LF capacitor voltage can be calculated as

$$\hat{v}_C = \frac{4\omega LMI_m}{16LC\omega^2 - (1-3D)^2} \quad (23)$$

3.6 Limitations of Capacitance and Inductance in the New PWM

Method

The capacitor and inductor is selected in qSBI based on the HF peak to peak voltage ripple in capacitor and HF peak to peak inductor current, the HF capacitor voltage is limited by $r_C\%$ and for HF inductor current is limited by $r_L\%$.

$$r_L\% = \frac{\Delta I_L}{I_L} \quad (24)$$

$$r_C\% = \frac{\Delta V_C}{V_C} \quad (25)$$

$$I_L = \frac{P_o}{V_{dc}} \quad (26)$$

By substituting these equations into HF inductor current and HF capacitor voltage equation (11) and (12) respectively the capacitance and inductance should be

$$\begin{cases} I_L r_L\% = \frac{V_{dc}(1-D)(1+3D)T}{2L(1-3D)} \\ V_C r_C\% = \frac{I_L(1+D)T}{4C} \end{cases}$$

$$\Rightarrow \begin{cases} \frac{P_o}{V_{dc}} r_L\% = \frac{V_{dc}(1-D)(1+3D)T}{2L(1-3D)} \\ \frac{2V_{dc}}{(1-3D)} r_C\% = \frac{P_o(1+D)T}{4C} \end{cases}$$

$$\begin{cases} L > \frac{V_{dc}^2(1-D)(1+3D)T}{2r_L\%(1-3D)P_o} \\ C > \frac{(1+D)(1-3D)TP_o}{8r_C\%V_{dc}^2} \end{cases} \quad (27)$$

If the inductance and capacitance are selected, it should verify the LF capacitor voltage and LF inductor current by substituting the selected capacitance and inductance into equations. If the peak values of LF ripple are not within the desired range, the

capacitance and the inductance can be increased until the peak value becomes within the desired range.

Chapter 4

SIMPLE BOOST CONTROL (SBC) FOR QUASI SWITCH

BOOST INVERTER (qSBI)

4.1 PWM Simple Boost Control Method for qSBI

The PWM Simple boost control method used in single-phase quasi switch boost inverter (qSBI) [10]. SBC PWM compare the high frequency triangle (dashed line) waveform (v_{tri_1}) and (v_{tri_2}) with a constant voltage (v_{SH}) to generate a control signal for S_5 . This shoot through control signal is inserted into H-bridge switches (S_1 - S_4) through OR logic gates to generate the shoot trough state to boost the voltage input. And two control waveforms v_{con} and $-v_{con}$ are compared with the high frequency triangle (dashed line) waveform (v_{tri_2}) to generate control signal for switches (S_1 - S_4) as it's shown in Figure 19.

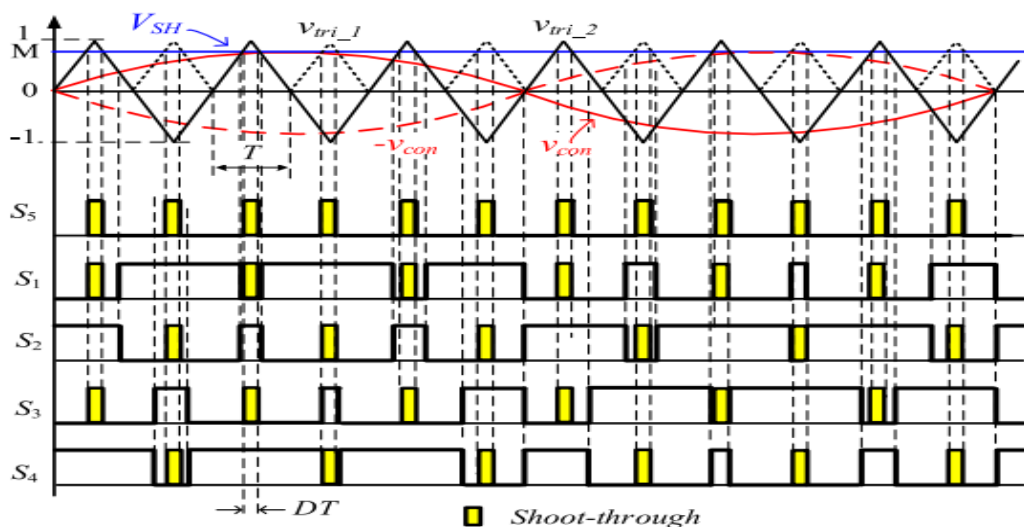


Figure 19: Simple Boost Control for Quasi Switch Boost Inverter [9]

The operating states are simplified into shoot-through and non-shoot-through states. Figure 20 shows the operating states and steady-state waveforms of the embedded-type qSBI. In the non-shoot-through state, as shown in Figure 20 (a), the inverter has two active states and two zero. The time interval in this state is $(1 - D) \cdot T$. During the non-shoot-through state, D_a and D_b are turned on, whereas S_5 is turned off. Capacitor C is charged from V_{dc} , whereas inductor L transfers energy from the dc voltage source to the main circuit. In the shoot-through state, as shown in Figure 20 (b), the inverter side is shorted by both the upper and lower switching devices of any phase leg. The time interval in this state is $D \cdot T$. During the shoot-through state, S_5 is turned on, whereas D_a and D_b are turned off. Capacitor C is discharged, whereas inductor L stores energy.

4.2 qSBI Circuit Analysis for SBC Method

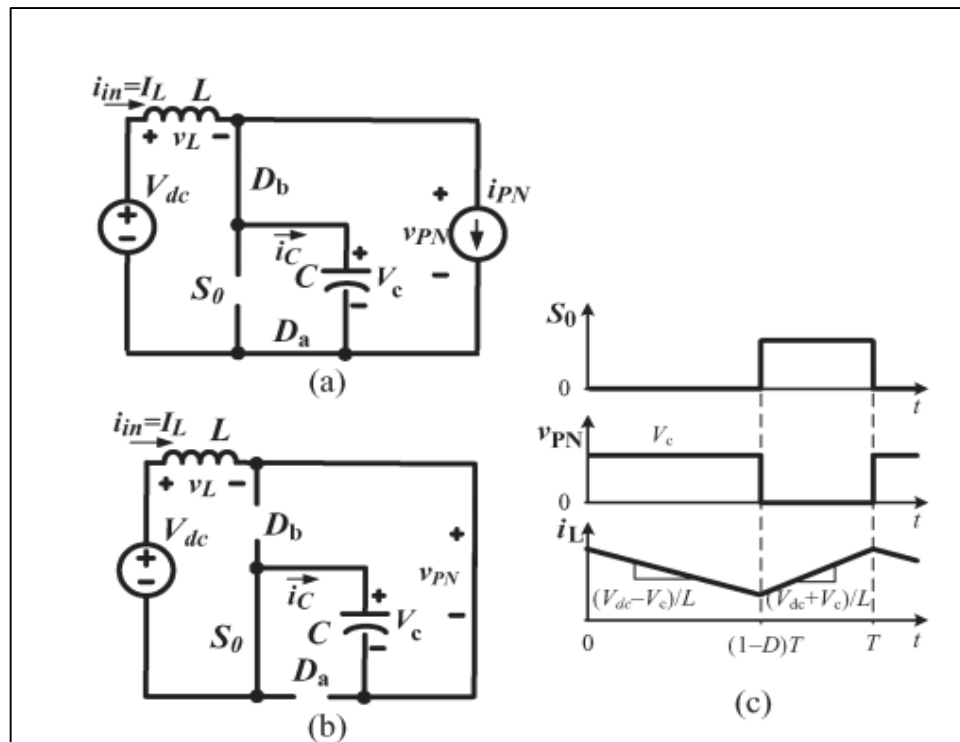


Figure 20: The Operating States of Simple Boots Converter for qSBI [10]

In the non-shoot-through state shown in Figure 20 (a), is obtained as.

$$\begin{cases} L \frac{di_L}{dt} = V_{dc} - V_C \\ C \frac{dV_C}{dt} = I_L - i_{PN} \end{cases} \quad (28)$$

In the shoot-through state shown in Figure 20 (b), we got

$$\begin{cases} L \frac{di_L}{dt} = V_{dc} + V_C \\ C \frac{dV_C}{dt} = -I_L \end{cases} \quad (29)$$

Applying the volt-second balance principle to L and C in the steady state (1) and (2).

$$\begin{cases} V_C = \frac{1}{1-2D_0} V_{dc} \\ i_{PN} = \frac{1-2D_0}{1-D_0} I_L \end{cases}$$

)30(

The peak dc-link voltage that crosses the inverter is expressed in the non-shoot-through state as.

$$V_{PN} = V_C = \frac{1}{1-2D_0} V_{dc} \quad (31)$$

The boost factor of the embedded-type qSBI is defined by

$$B_E = \frac{V_{PN}}{V_{dc}} = \frac{1}{1-2D_0} \quad (32)$$

4.3 PWM Control of qSBI for SBC

The peak value of the output voltage is given by

$$\hat{v}_o = M_0 \cdot V_{PN} = M_0 \cdot B \cdot V_{dc} \quad (33)$$

The dc-ac inversion voltage gain is defined by

$$G = M_0 \cdot B = \frac{\hat{v}_o}{V_{dc}} \quad (34)$$

The sum of the shoot-through duty ratio and the modulation index must be less than 1 to ensure that the shoot-through interval is only inserted into the traditional zero states. Thus, the maximum duty cycle of the shoot-through state is $(1 - M)$ the voltage gain (G) define as.

$$G = M_0 \cdot B_E = \frac{M_0}{2M_0 - 1} \quad (35)$$

4.4 High Frequency Peak to Peak Capacitor Voltage and Inductor Current under SBC Control Method

Figure 21 shows the high frequency (HF) peak to peak inductor current and capacitor voltage for SBC method in non-shoot through is given by [10]

$$\begin{cases} \Delta I_{L_SBC} = \frac{2V_{dc}D_0(1-D_0)T}{L(1-2D_0)} \\ \Delta V_{C_SBC} = \frac{I_L D_0 T}{C} \end{cases} \quad (36)$$

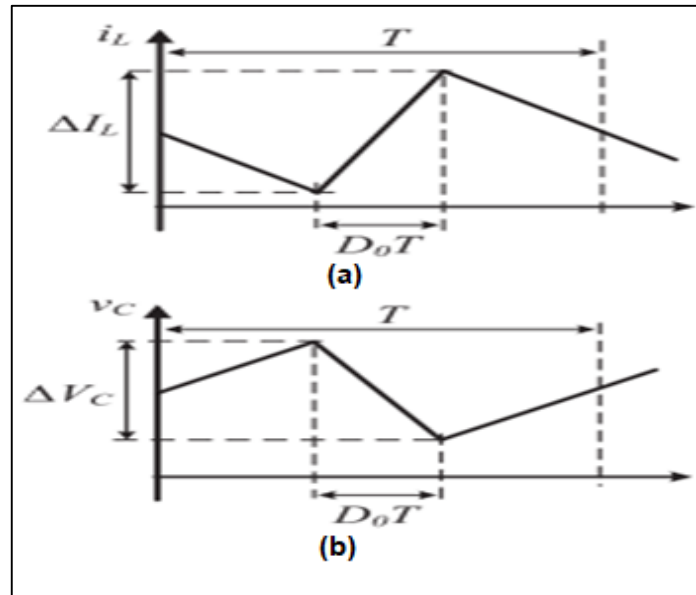


Figure 21: High Frequency (HF) Peak to Peak Inductor Current and Capacitor Voltage for SBC Method [9]

4.5 AC Component Circuit Analysis for Simple Boost Control (SBC)

It is obtained in shoot-through

$$\begin{cases} L \frac{d\hat{i}}{dt} = \hat{v}_C \\ C \frac{d\hat{v}_C}{dt} = -\hat{i}_L \end{cases} \quad (37)$$

In non-shoot through state obtained as

$$\begin{cases} L \frac{d\hat{i}}{dt} = -\hat{v}_C \\ C \frac{d\hat{v}_C}{dt} = -\hat{i}_L - \hat{i}_{PN_non} \end{cases} \quad (38)$$

By applying small signal analysis method, the state-space averaged model of the simplified qSBI is obtained as

$$\begin{cases} L \frac{d\hat{i}}{dt} = (D_0 + \hat{d}) \cdot (v_C) + (1 - D_0 - \hat{d}) \cdot (-\hat{v}_C) \\ C \frac{d\hat{v}_C}{dt} = (D_0 + \hat{d}) \cdot (-i_L) + (1 - D_0 - \hat{d}) \cdot (\hat{i}_L - \hat{i}_{PN_non}) \end{cases} \quad (39)$$

Replace equation (39) to frequency domain 2ω as follows

$$\begin{cases} j2\omega \hat{i}_L = -(1 - 2D_0) \cdot \hat{v}_C + 2V_C \cdot \hat{d} \\ j2\omega C \hat{v}_C = (1 - 2D_0) \cdot \hat{i}_L - (1 - D_0) \cdot \hat{i}_L - (1 - D_0) \cdot i_{PN_non} + (I_{PN_non} - 2I_L) \cdot \hat{d} \end{cases} \quad (40)$$

The small signal in the shoot through duty cycle (\hat{d}) can be minimized through reasonable control design and the effect of \hat{d} for LF ripples of the capacitor voltage and inductor current is less important than that of the dc link LF current ripples i_{PN_non} . The small signal perturbation of the shoot through should be ignored .so solving equation (40) with $\hat{d} = 0$ the LF 2ω inductor current and capacitor voltage can be defined as

$$\begin{cases} \hat{i}_L = \frac{(1-2D_0)M_0 \cos(2\omega t - \varphi)}{4LC\omega^2 - (1-2D_0)^2} \\ \hat{v}_C = \frac{\omega LM_0 I_M \sin(2\omega t - \varphi)}{4LC\omega^2 - (1-2D_0)^2} \end{cases}$$

The magnitude of the Peak value of LF inductor current \hat{i}_L and the Peak value of LF capacitor voltage \hat{V}_C is defined as

$$\begin{cases} \hat{i}_L = \frac{(1-2D_0)M_0}{4LC\omega^2 - (1-2D_0)^2} \\ \hat{v}_C = \frac{\omega LM_0 I_M}{4LC\omega^2 - (1-2D_0)^2} \end{cases} \quad (41)$$

Chapter 5

COMPARISON BETWEEN THE SBC METHOD AND THE NEW PWM CONTROL METHOD

5.1 The Relation between The Boost Factor in the SBC and New PWM Methods

Under the new method for qSBI the boost factor is very high compared to the conventional SBC method as shown in Figure 22. B_p is the boost factor for the new and B_s for the conventional SBC Method.

$$\begin{cases} B_p = \frac{2}{1-3D} \\ B_s = \frac{1}{1-2D_0} \end{cases} \quad (42)$$

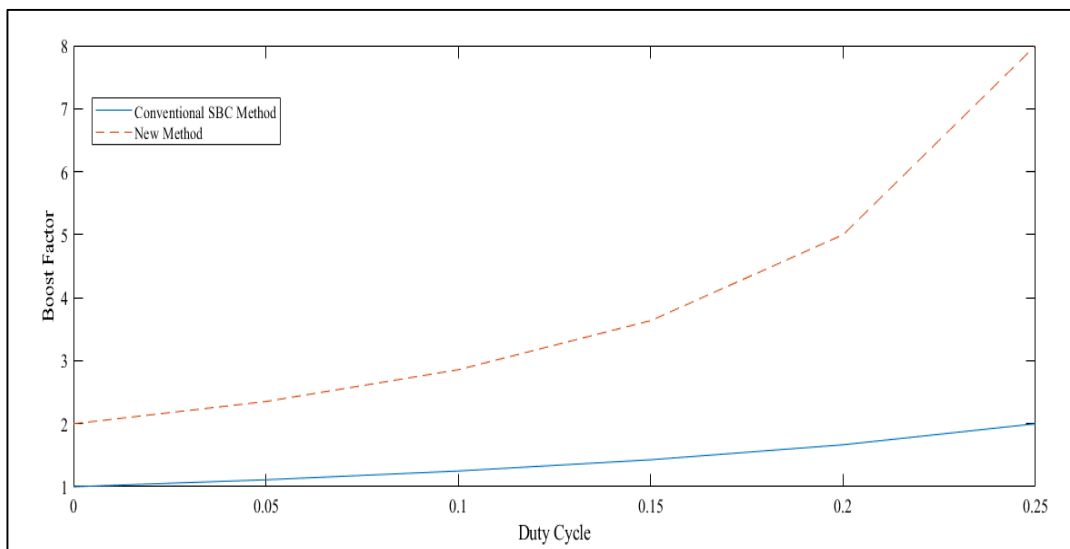


Figure 22: Boost Factor Comparison between the Two Methods

5.2 The Relation between The Modulation Index in the SBC and New PWM Methods

$$\begin{cases} G_p = M \cdot B_p = \frac{2M}{3M-2} \\ G_s = M \cdot B_s = \frac{M_0}{2M_0-1} \end{cases} \quad (43)$$

The new PWM control uses a high modulation index as shown Figure 23 in to improve the output voltage gain. For the same voltage gain from equation (43) it ensure that the modulation index for the SBC control method is M_0 and the modulation index for new PWM control method defined as

$$\begin{aligned} G_s &= \frac{M_0}{2M_0-1} = G_p = \frac{2M}{3M-2} \\ \Rightarrow 3MM_0 - 2M_0 &= 4MM_0 - 2M \\ \Rightarrow 2M - MM_0 &= 2M_0 \\ M &= \frac{2M_0}{2-M_0} > M_0 \end{aligned} \quad (44)$$

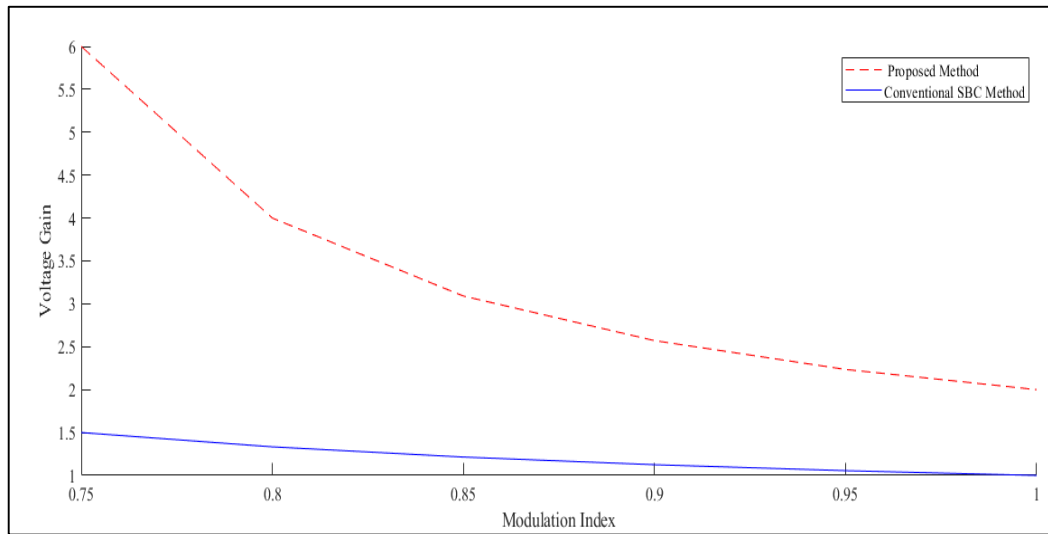


Figure 23: Voltage Gain Comparison between the Two Methods

5.3 The Relation between The Duty Cycle in the SBC and New PWM

Methods

From, equation (43) the relationship between the shoot through duty cycle (D) in the new PWM method and the SBC method shoot through duty cycle (D_0) for the same voltage gain is defined by

By substituting $M = (1-D)$ and $M_0 = (1-D_0)$

$$\Rightarrow 1-D = \frac{2(1-D_0)}{2-(1-D_0)}$$

$$\Rightarrow 1-D = \frac{2(1-D_0)}{1+D_0}$$

$$\Rightarrow (1-D)(1+D_0) = 2-2D_0$$

$$\Rightarrow 1+D_0-D-DD_0 = 2-2D_0$$

$$\Rightarrow 3D_0-DD_0 = 1+D$$

$$D_0 = \frac{1+D}{3-D} \tag{45}$$

5.4 Comparing the High Frequency Peak to Peak Capacitor Voltage and Inductor Current of the Conventional SBC Method and the New Method

By Substituting D_0 of equation (45) into equation (36) we will compare ΔI_{L_SBC} and ΔV_{C_SBC} to the new method in equation (11) and (12) to see that the high frequency peak to peak inductor current and the HF peak to peak capacitor voltage in the new method are lower than those in SBC method.

So substitute D_0 from equation (45) into ΔV_{C_SBC} equation (36)

$$\Delta V_{C_SBC} = \left(\frac{I_L \left(\frac{1+D}{3-D} \right) T}{C} \right)$$

Comparing it with the ΔV_C equation (12) of the new method, normalize it by $V_B = \frac{I_L T}{C}$

,The HF peak to peak capacitor voltage for the two methods are defined as

$$\left\{ \begin{array}{l} \left(\frac{1+D}{3-D} \right)_{SBC} \\ \left(\frac{1+D}{4} \right)_{NEW} \end{array} \right. \quad (46)$$

Thus, it is recognized that HF peak to peak capacitor voltage in the new method is lower than those in SBC method as shown in Figure 24.

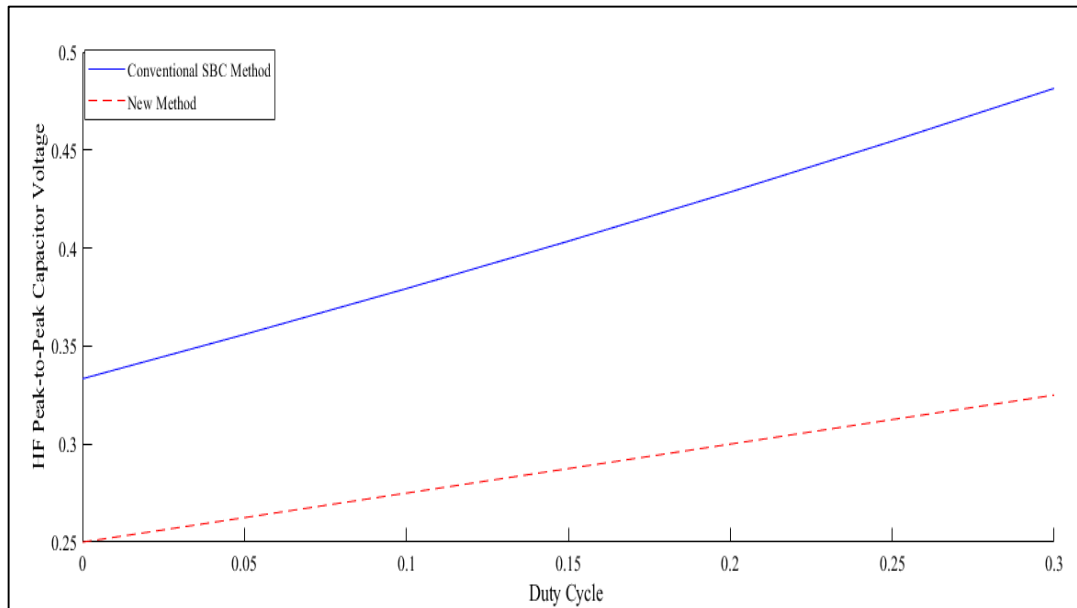


Figure 24: HF Peak to Peak Capacitor Voltage Comparison between the Two Methods

For HF peak to peak inductor current by substituting D_0 equation (45) into ΔI_{L_SBC} equation (36)

$$\Delta I_{L_SBC} = \frac{2V_{dc} \left(\frac{1+D}{3-D} \right) \left(1 - \left(\frac{1+D}{3-D} \right) T \right)}{\left(L \left(1 - 2 \left(\frac{1+D}{3-D} \right) \right) \right)}$$

$$\Delta I_{L_SBC} = \frac{4V_{dc} T}{L} \left(\frac{(1+D)(1-D)}{(3-D)(1-3D)} \right)$$

And by comparing it with ΔI equation (11) of the new method, normalize it by

$I_B = \frac{V_{dc} T}{L}$, The HF peak to peak inductor current for the two methods are defined as

$$\left\{ \begin{array}{l} \left(\frac{4(1-D^2)}{(3-D)(1-3D)} \right)_{SBC} \\ \left(\frac{(1-D)(1+3D)}{(1-3D)} \right)_{NEW} \end{array} \right. \quad (47)$$

It is recognized that HF peak to peak inductor current in the new method is lower than those in SBC method as shown in Figure 25.

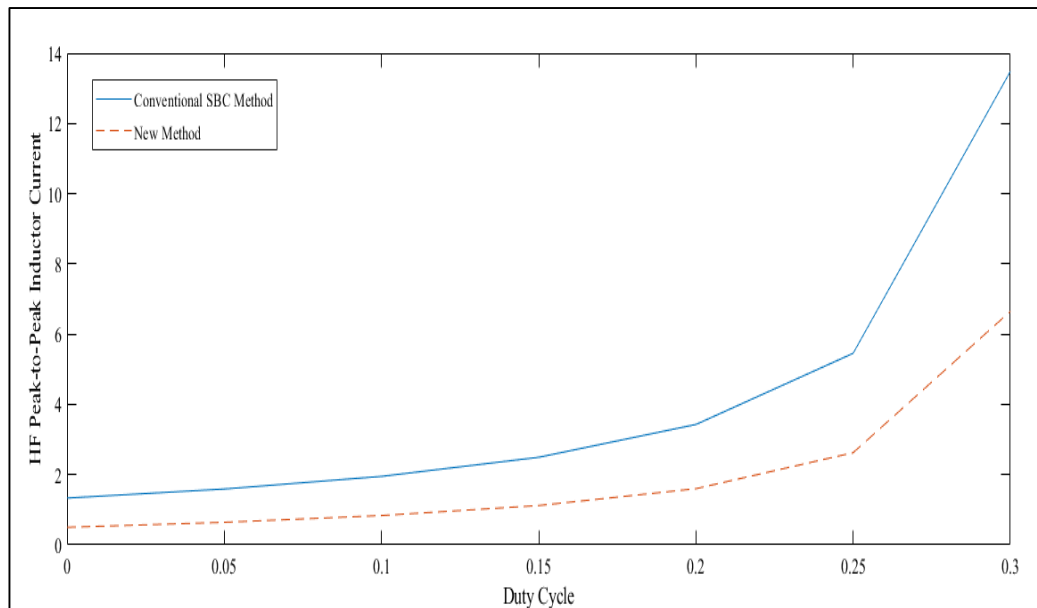


Figure 25: HF Peak to Peak Inductor Current Comparison between the Two Methods

5.5 Governing the Equations of the SBC and the New PWM Methods

The comparison between the governing equations of the SBC method and the new method for the single phase qSBI is shown in Table 1.

Table 1: Comparison between the Covering Equations of the SBC Method and New Method

| | SBC | New method |
|---|---|---|
| Capacitor voltage V_C | $\frac{V_{dc}}{1-2D_0}$ | $\frac{2V_{dc}}{1-3D_0}$ |
| DC-Link voltage V_{PN} | V_C | V_C |
| Switch and Diode voltage stress | V_C | V_C |
| Voltage gain G | $\frac{M_0}{2M_0-1}$ | $\frac{3M}{3M-2}$ |
| Average inductor current | $\frac{P_o}{V_{dc}}$ | $\frac{P_o}{V_{dc}}$ |
| HF peak to peak inductor ripple current ΔI_L | $\frac{2V_{dc}D_0(1-D_0)T}{L(1-2D_0)}$ | $\frac{T}{2L}V_{dc} \frac{(1-D)(1+3D)}{(1-3D)}$ |
| HF peak to peak capacitor ripple voltage ΔV_C | $\frac{I_L D_0 T}{C}$ | $\frac{T}{4C}(1+D)I_L$ |
| Peak value of LF inductor current \hat{i}_L | $\frac{(1-2D_0)\hat{i}_{PN_non}}{2(4LC\omega^2-(1-2D_0)^2)}$ | $\frac{(1-3D)\hat{i}_{PN_non}}{16LC\omega^2-(1-3D)^2}$ |
| Peak value of LF capacitor voltage \hat{v}_C | $\frac{\omega LM_0 I_M}{4LC\omega^2-(1-2D_0)^2}$ | $\frac{4\omega L M I_M}{16LC\omega^2-(1-3D)^2}$ |

5.6 Theoretical Results

By comparing the stresses between both methods, it is noticed that the voltage stress on the dc-link diodes capacitors and switches in the conventional SBC method is higher than that of the new PWM control method by using parameters in Table 2.

Table 2: Parameters for the New PWM Method and SBC

| Parameter | Values |
|------------------------------|---------------|
| Input voltage range V_{dc} | 58 V |
| Output voltage \hat{v}_o | 175 V |
| Rated output power P_o | 400 W |
| Inductor L | 3 mH |
| Capacitor C | 680 μ F |
| The period T | 50 μ s |

By using Parameters for the new PWM method and SBC in Table 2 the theoretical result is as shown in Table 3.

Table 3: Theoretical Results for the New PWM Method

| | SBC | New method |
|--------------------------|------------|-------------------|
| Modulation index | 0.6 | 0.85 |
| Shoot-through duty cycle | 0.4 | 0.15 |
| Diode voltage stress | 290 | 290 |
| Capacitor voltage | 290 | 290 |
| Switch voltage stress | 290 | 290 |

| | | |
|--|--------|--------|
| Average inductor current | 6.9 A | 6.9 A |
| HF peak to peak capacitor ripple voltage | 0.21 V | 0.15A |
| HF peak to peak inductor ripple current | 2.32 A | 1.08 A |
| Peak value of LF capacitor voltage | 3.4 V | 5.0 V |
| Peak value of LF inductor voltage | 0.36A | 0.73A |

The advantage of PWM method is greater than that of the conventional SBC method. It reduces the voltage stress, improves the modulation index, lowers the peak to peak inductor current and lowers the capacitor voltage ripple and shoot through current. The disadvantage of the new PWM is that the peak values of LF inductor current and the LF capacitor voltage are higher than those of the SBC method.

Chapter 6

SIMULATION AND RESULT FOR THE NEW PWM AND SBC METHODS

6.1 Introduction

This chapter addresses the comparison simulation results of the new and the SBC methods using the Simulink Matlab model of these methods. As shown in Figure 26 This model consists of the topology for quasi switch boost inverter (qSBI) for the two methods with RL load. The topology is constructed to give the reader the ability to understand how the model works. It uses the measurement devices available in the Simulink to measure and plot all the required outputs of the model.

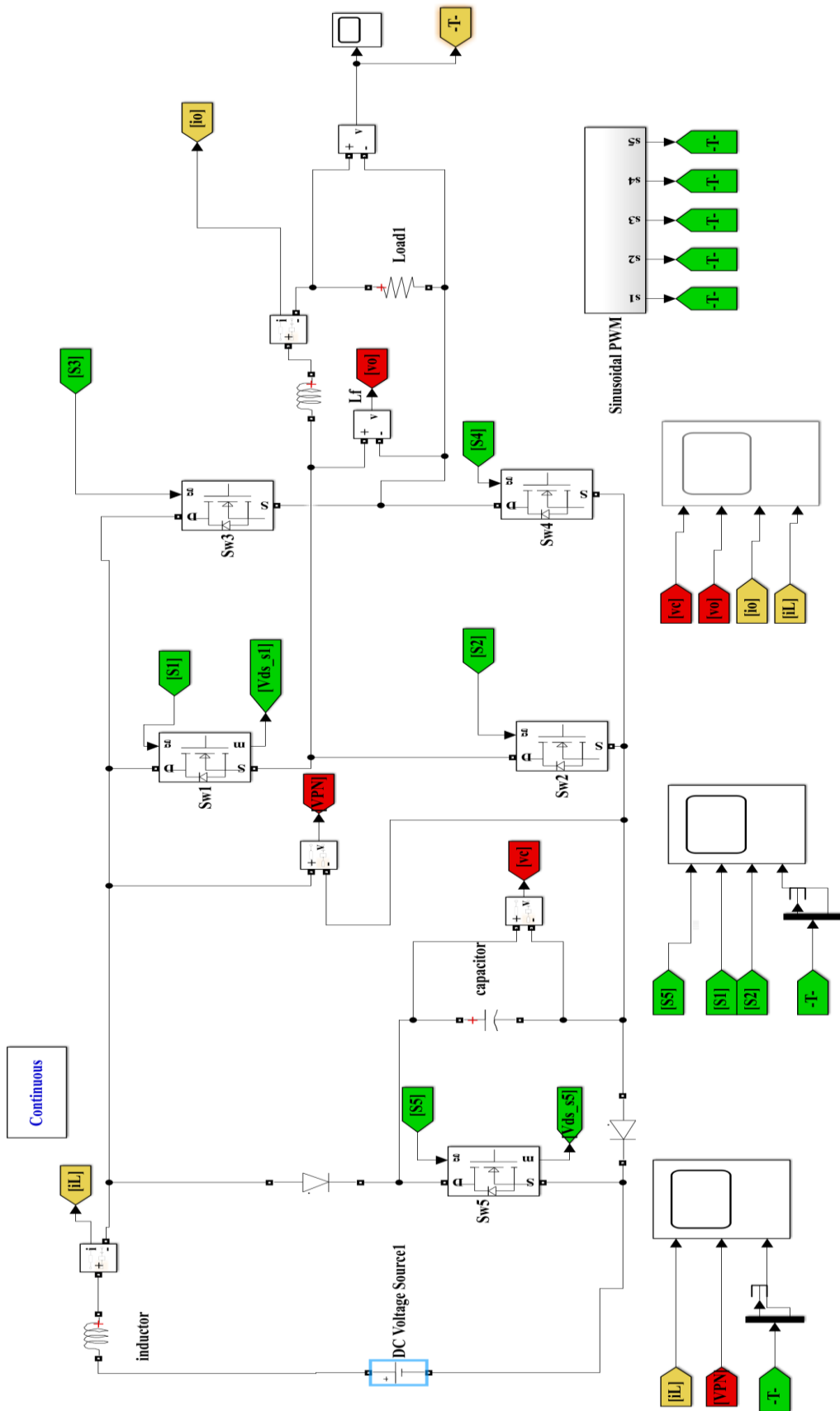


Figure 26 : The Topology of the New PWM and SBC Methods

The parameters of the system simulated in Matlab-simulink are in Table 4.

Table 4: Parameter Used For Simulink

| Parameter | Values |
|---|---|
| Input voltage range V_{dc} | 58 V |
| Rated output power P_0 | 400 W |
| Output voltage V_0 | $110 V_{rms} / 50\text{Hz}$ |
| Maximum input current (I_L) | 10A |
| Capacitor C | 680 μF |
| Inductor L | 3 mH |
| Switching frequency of $S_1 \sim S_4$ | 10KHz |
| Switching frequency of S_5 | 20 KHz |
| Modulation index (M) | 0.85 with the New method 0.6 with the SBC method |
| Passive load $\begin{matrix} L \\ R \end{matrix}$ | 5mH 30 Ω |

6.2 Control Method Simulink Model

The switching logic for control signal generation for SBC method is shown in Figure 27. It is constructed in sub-block and saved in output port of the model to control all the 5 switches. A constant voltage shoot through is compared with a high frequency triangular1 waveform to generate shoot through control signal for switch 5 and used triangular2 to generate control signal for switch 1-4. For the new PWM in Figure 28.

A constant voltage shoot through is compared with a high frequency triangular¹ to generate shoot through control signal for switch 5 waveform, sawtooth triangle for the duty ratio of switch 5 and used triangle 2 to generate control signal for switch 1-4.

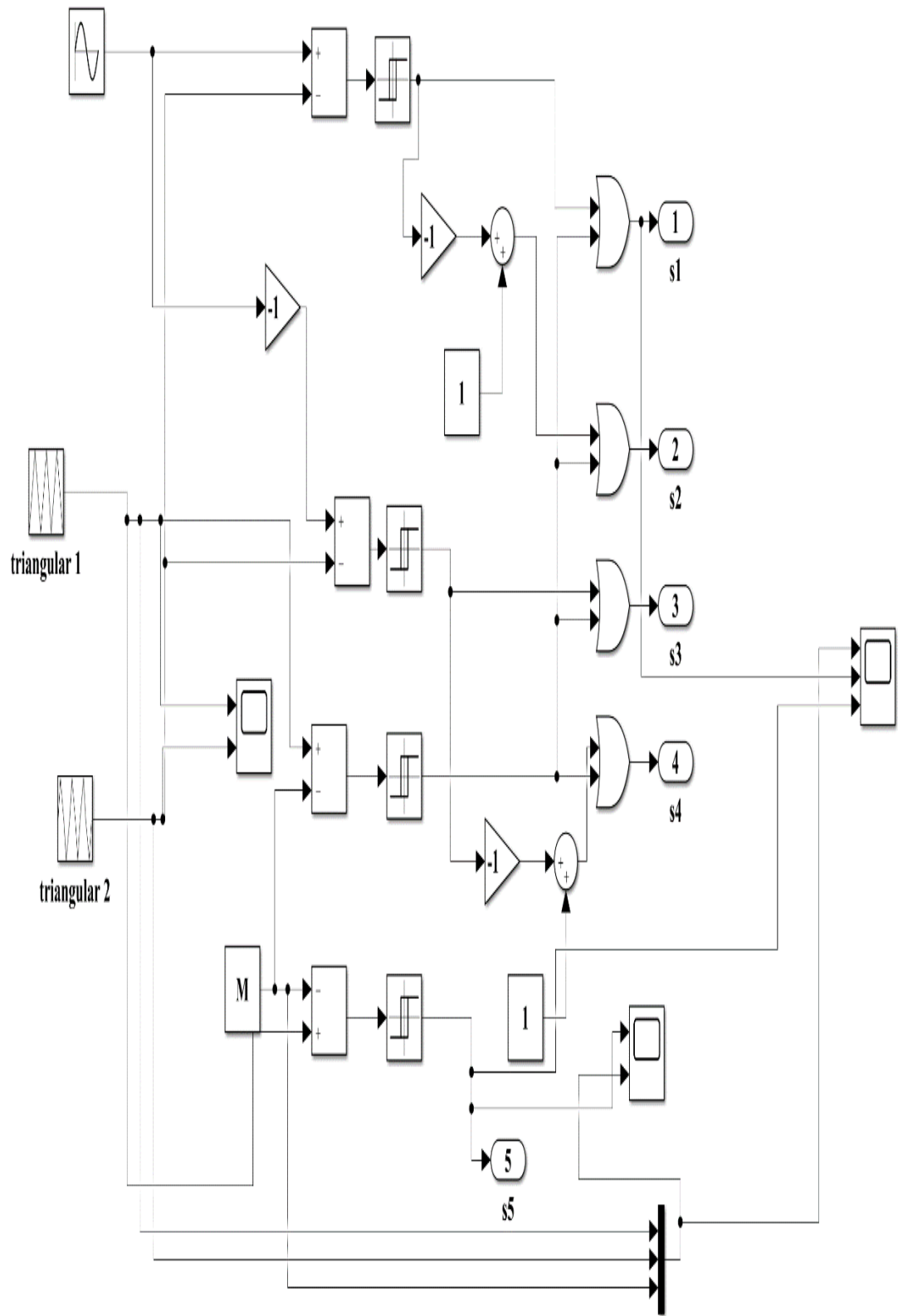


Figure 27: The Model Control of the SBC Method

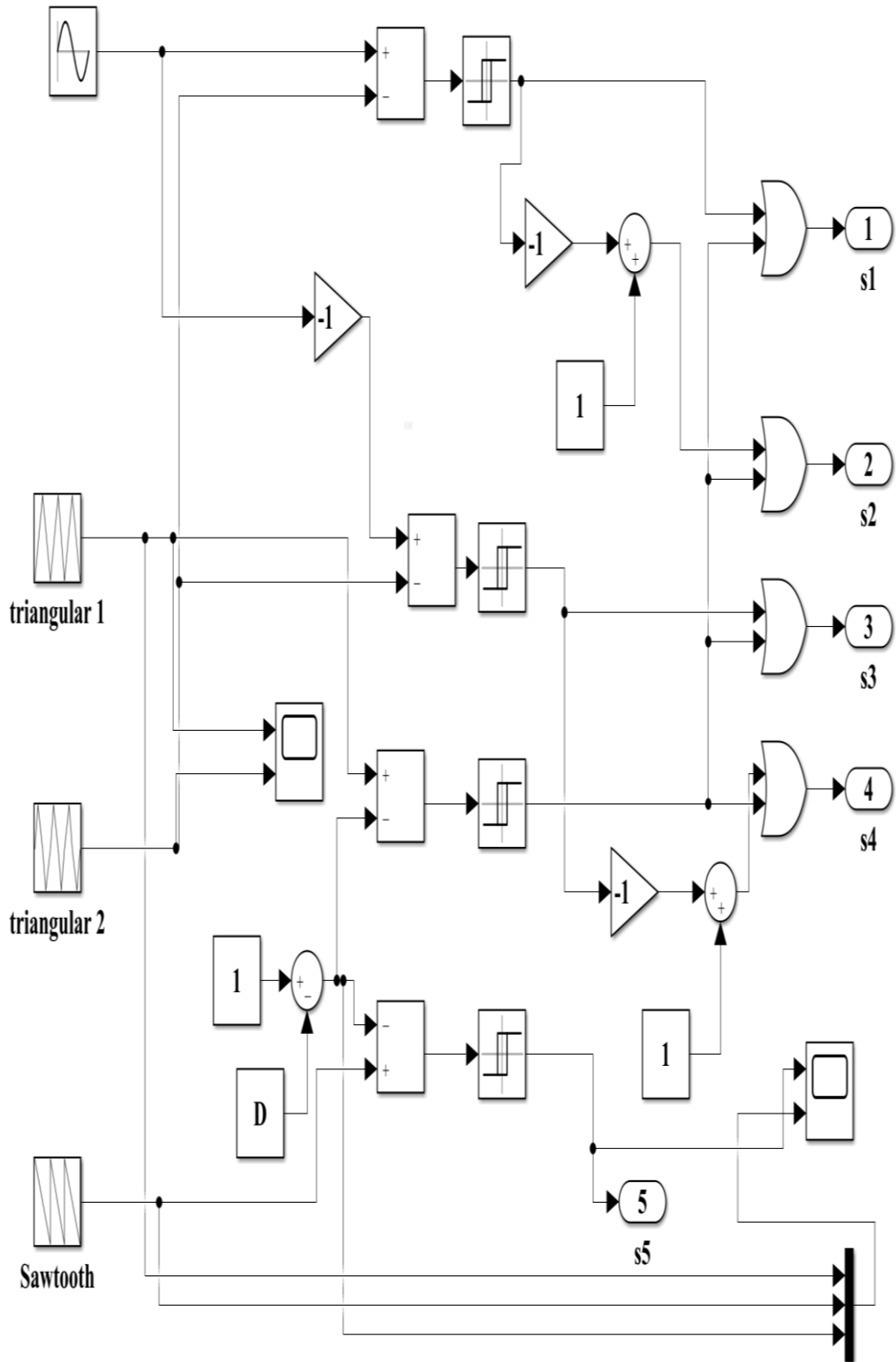


Figure 28: The Model Control of the New PWM Method

6.2 Simulation Result

The simulation result for the SBC and the new PWM method is to obtain the input voltage, capacitor voltage, V_{dc} inductor current, the output voltage, control gate signal for the switches and drain source voltage of switch 1 and the output current and its harmonics.

6.2.1 Simulation Result of New PWM Method

Simulink-Matlab results of the quasi switched boost inverter (qSBI) under the new PWM method will study the two states.

6.2.1.1 Simulink Result of the New PWM Method State 1

Simulink Result of Nominal Load Test for the New PWM Method State 1

State 1 shows the Simulink results for new PWM control method when $M = 0.85$, $D = 0.15$ and $V_{dc} = 58 \text{ V}$.

The RMS output voltage is equal to 110V as shown in Figure 29

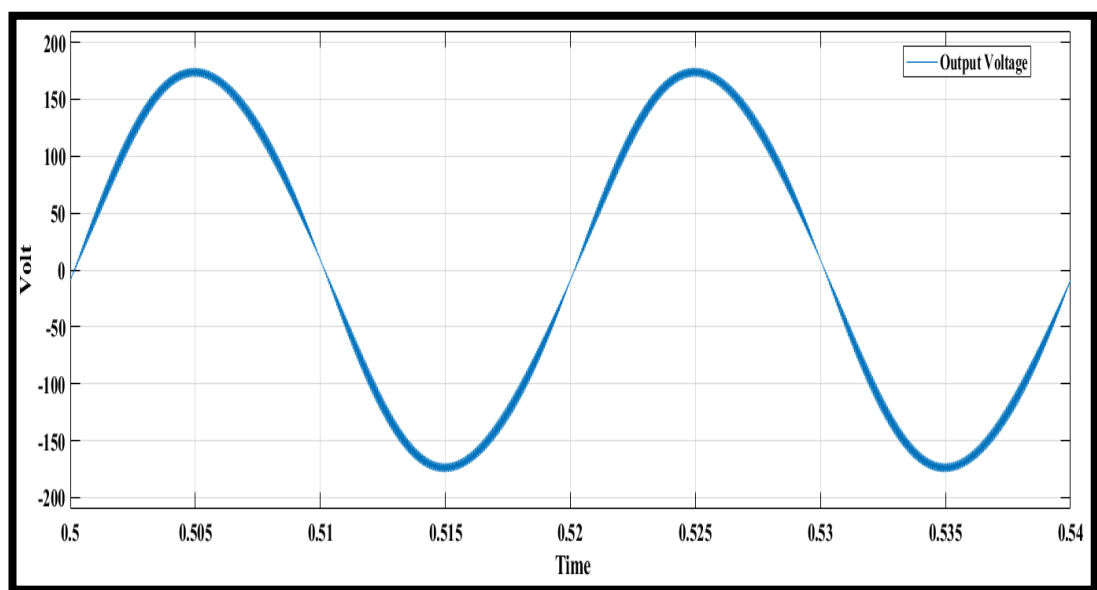


Figure 29: Output Voltage of the New PWM Method State 1

The peak capacitor voltage is equal to 211V as shown in Figure 30

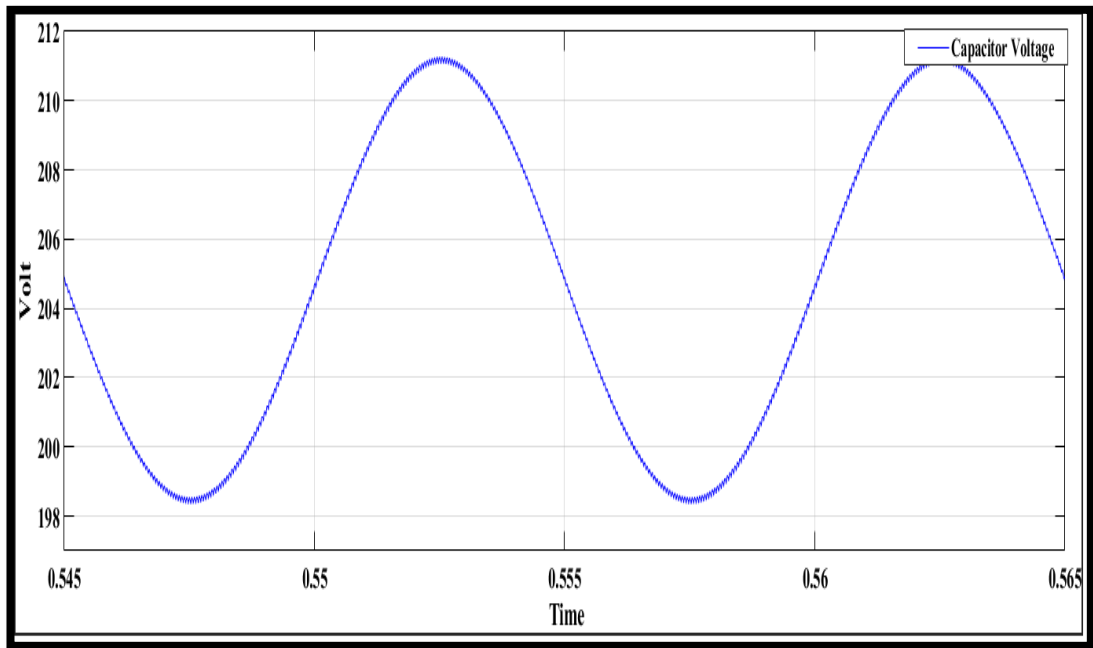


Figure 30: Capacitor Voltage of the New PWM Method State 1

The Vdc link voltage is equal to 2011 as shown in Figure 31

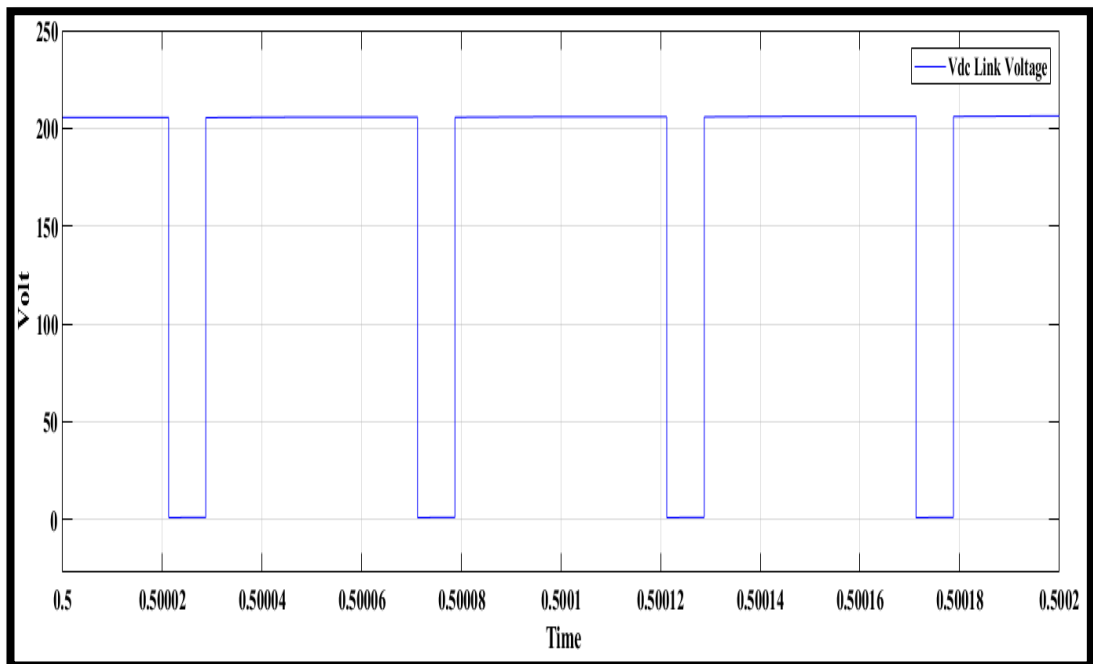


Figure 31: Vdc Link Voltage of the New PWM Method State 1

The high frequency peak to peak inductor current equal to 1.1A as shown in Figure 32

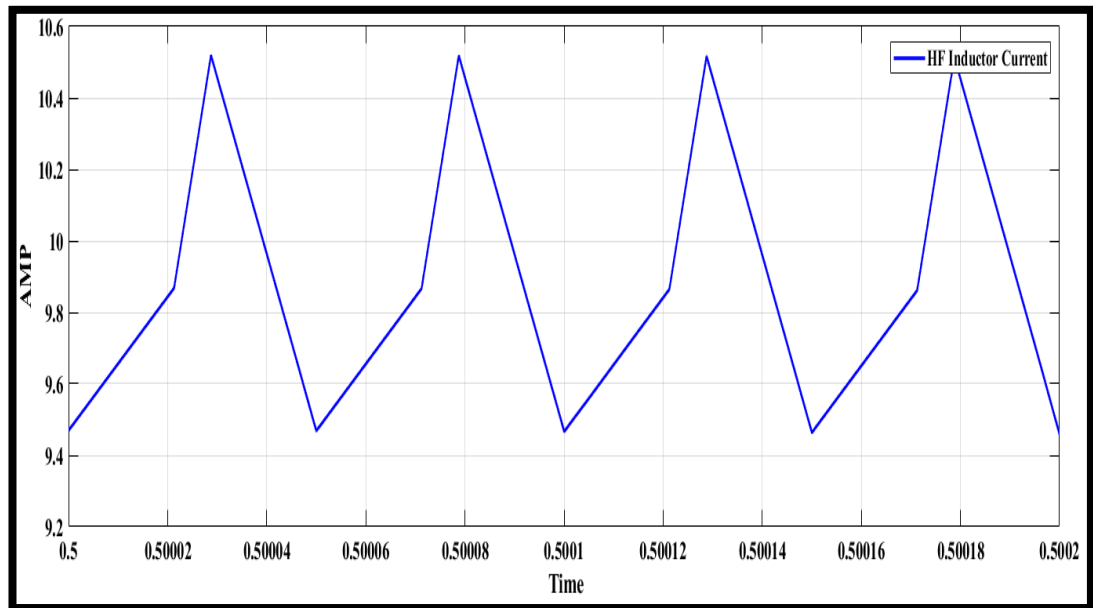


Figure 32: HF Inductor Current of the New PWM Method State 1

The high frequency peak to peak capacitor voltage equal to 0.2 as shown in Figure 33

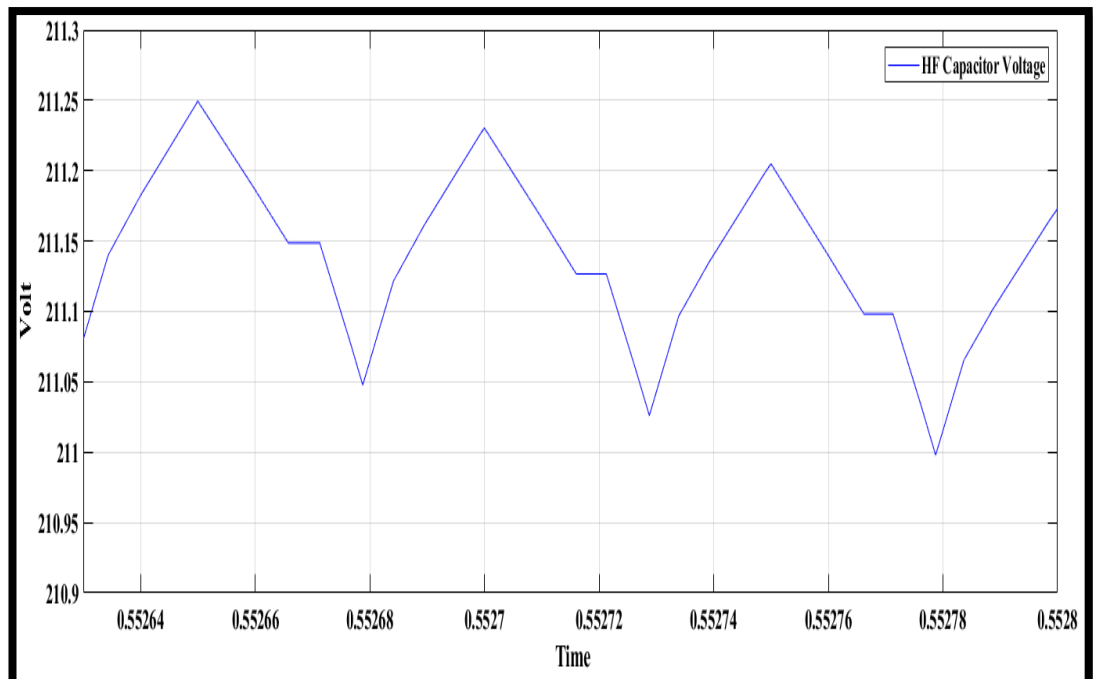


Figure 33: HF Capacitor Voltage of the New PWM Method State 1

The average inductor current is equal to 9A as shown in Figure 34

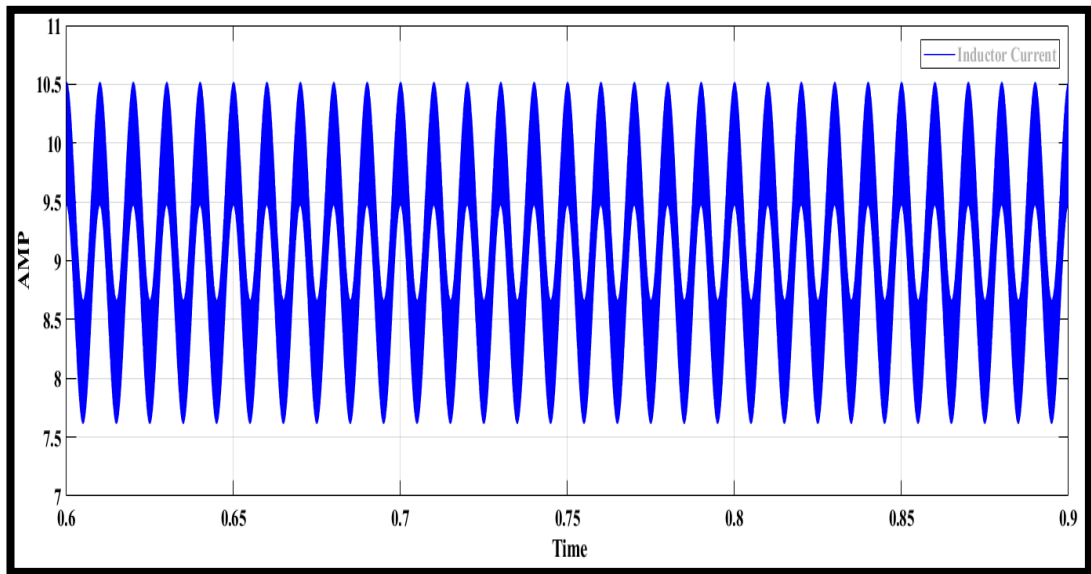


Figure 34: Average Inductor Current of the New PWM Method State 1

The peak value of low the frequency inductor current is equal to 0.88A as shown in Figure 35

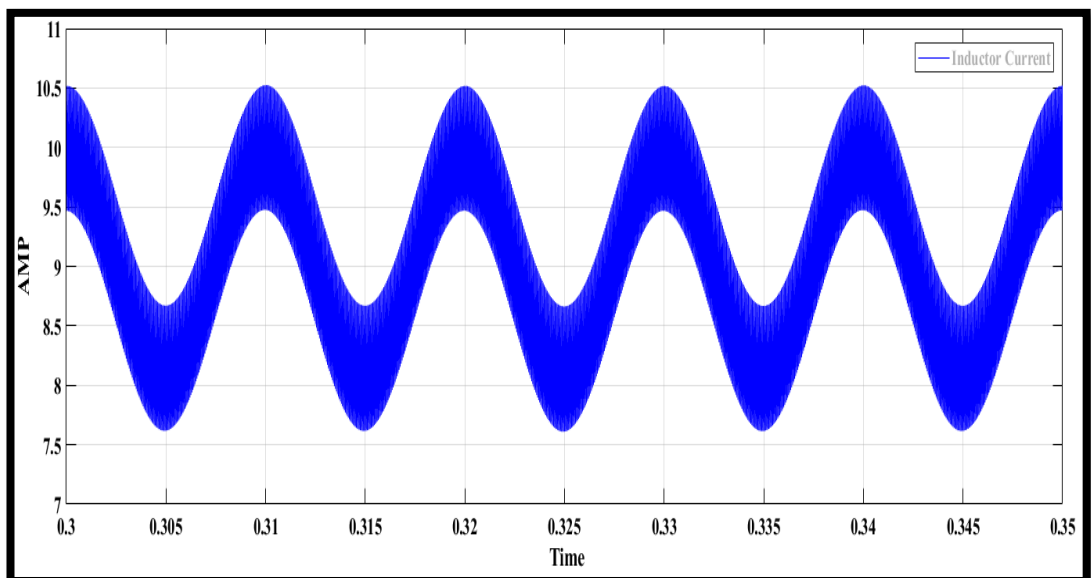


Figure 35: LF inductor current of the New PWM Method State 1

The peak value of low the frequency capacitor voltage is equal to 6V as shown in Figure 36

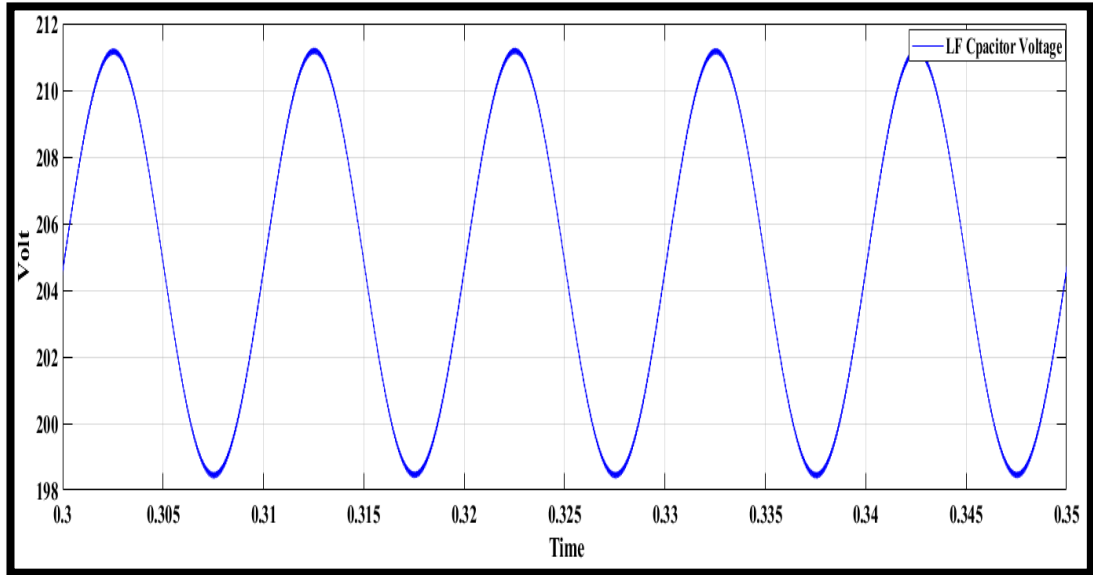


Figure 36: LF Capacitor Voltage of the New PWM Method State 1

The peak drain to source voltage of switch 5 is equal 211V as seen in Figure 37

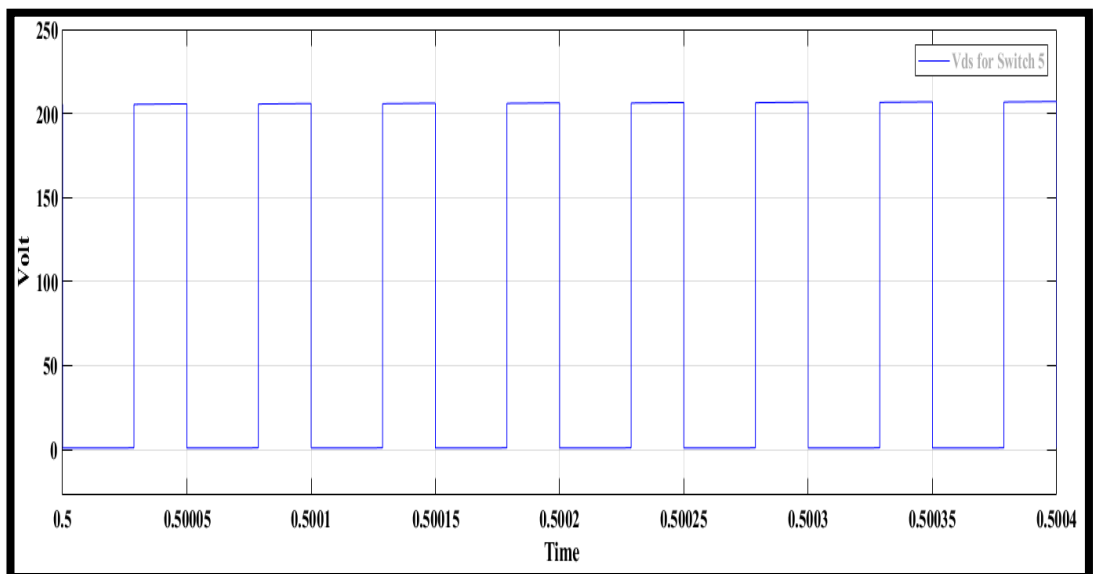


Figure 37: Vds Voltage of Switch 5 of the New PWM Method State 1

The peak drain to source voltage of switch 1 is equal 211V as seen in

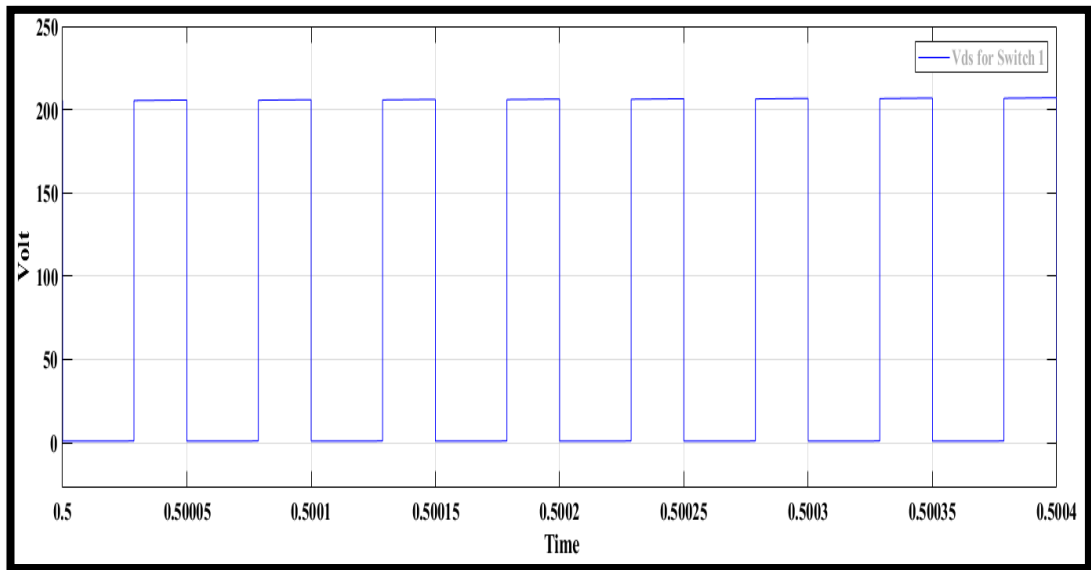


Figure 38: Vds Voltage of Switch 1 of the New PWM Method State 1

The RMS output current is equal 3.9A as shown in Figure 39

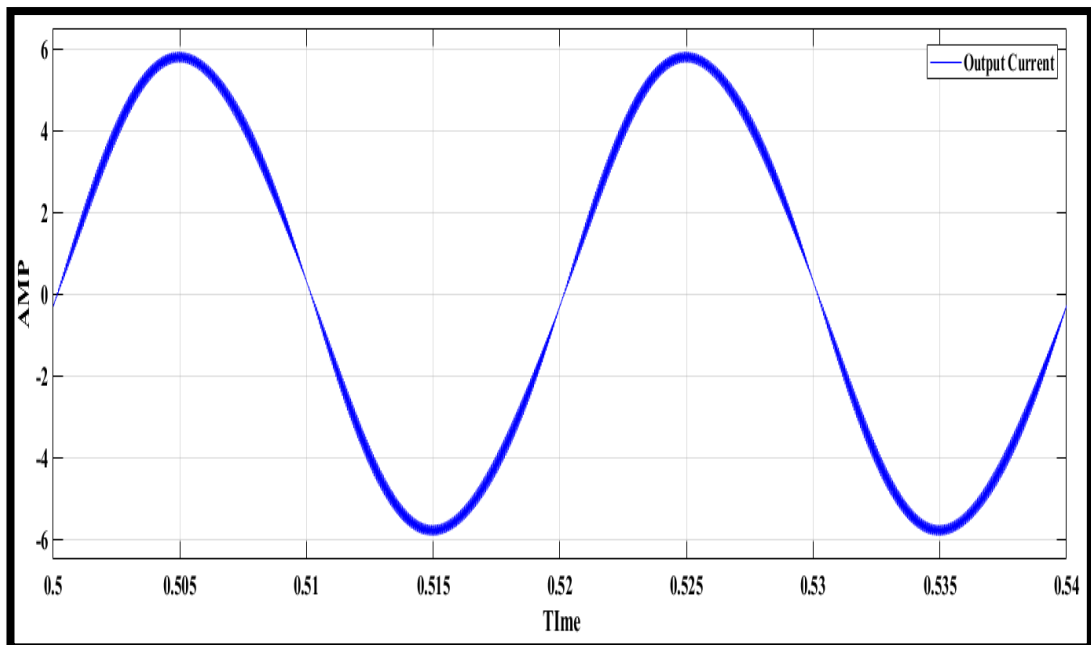


Figure 39: Output Current of the New PWM Method State 1

The THD output current is equal 3.14% as shown in Figure 40

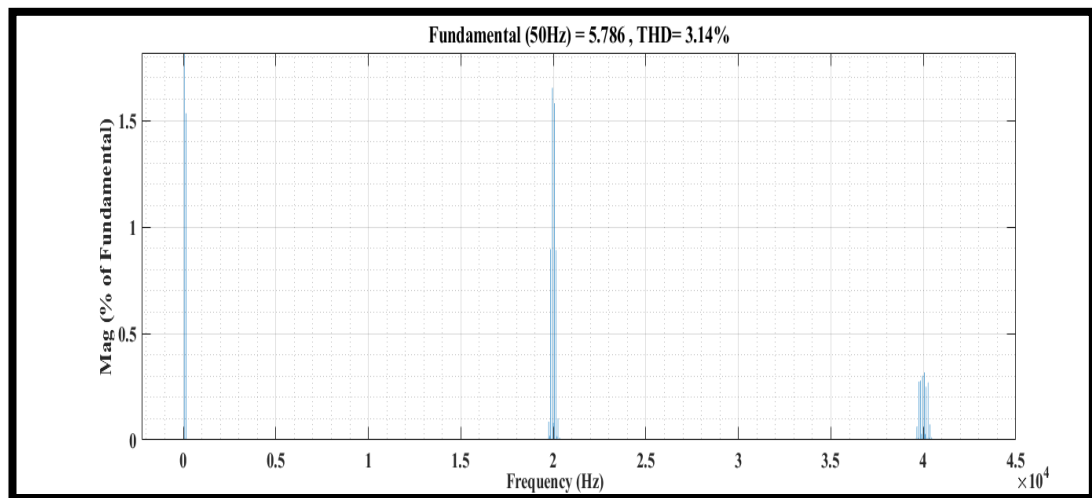


Figure 40: THD Output Current of the New PWM Method State 1

Simulink Result of Load Change Test for The New PWM Method State1

By changing the load from 30Ω to 15Ω , there is a small voltage dip in the capacitor voltage and in the output voltage waveform. And there is a small current dip in the output current and inductor current it is important to point that the system is not working in feed forward control where there is no feedback from the output voltage .

The output voltage of the load changing is shown in Figure 41

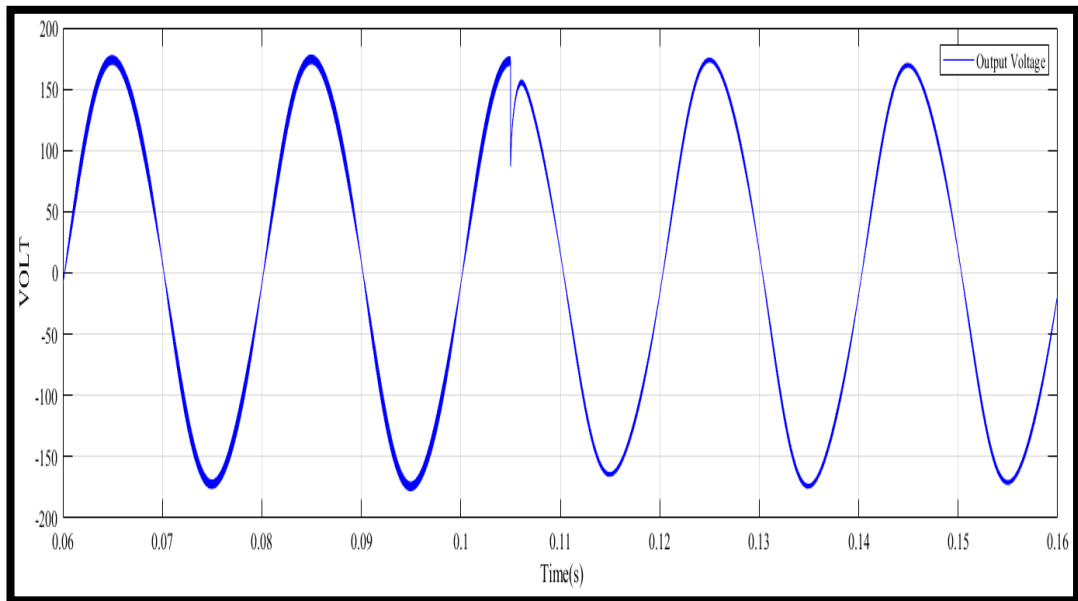


Figure 41: Output Voltage of Load Changing for the New PWM Method State 1

The output Current of the load changing is shown in Figure 42

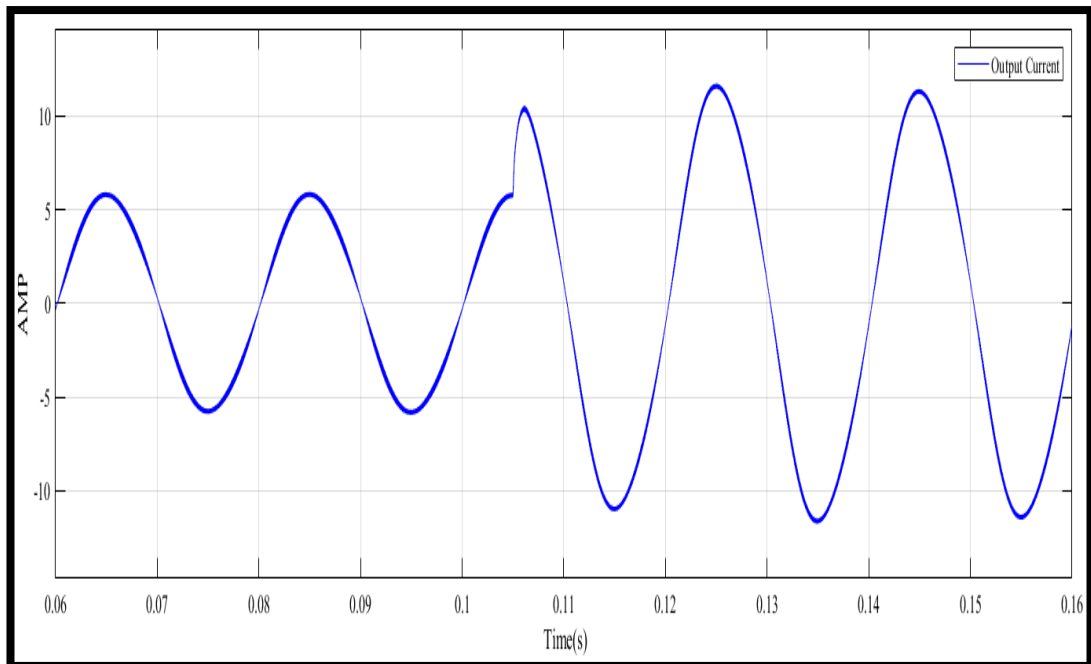


Figure 42: Output Current of Load Changing for the New PWM Method State 1

The capacitor voltage of the load changing as shown in

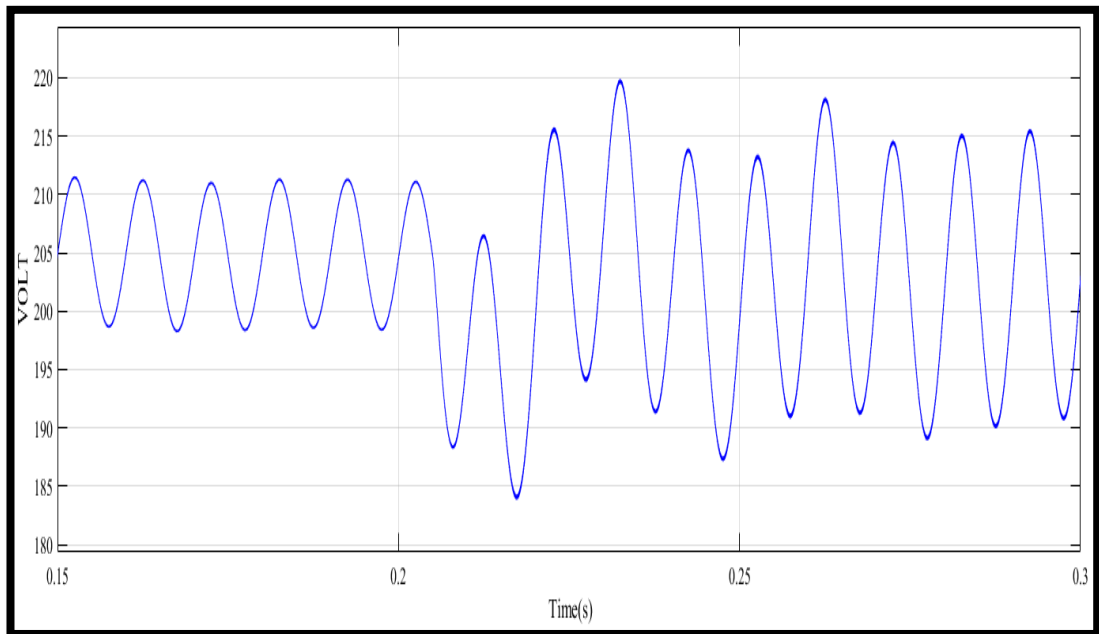


Figure 43: Capacitor Voltage of Load Changing for the New PWM Method State 1

The inductor current of load changing is shown in

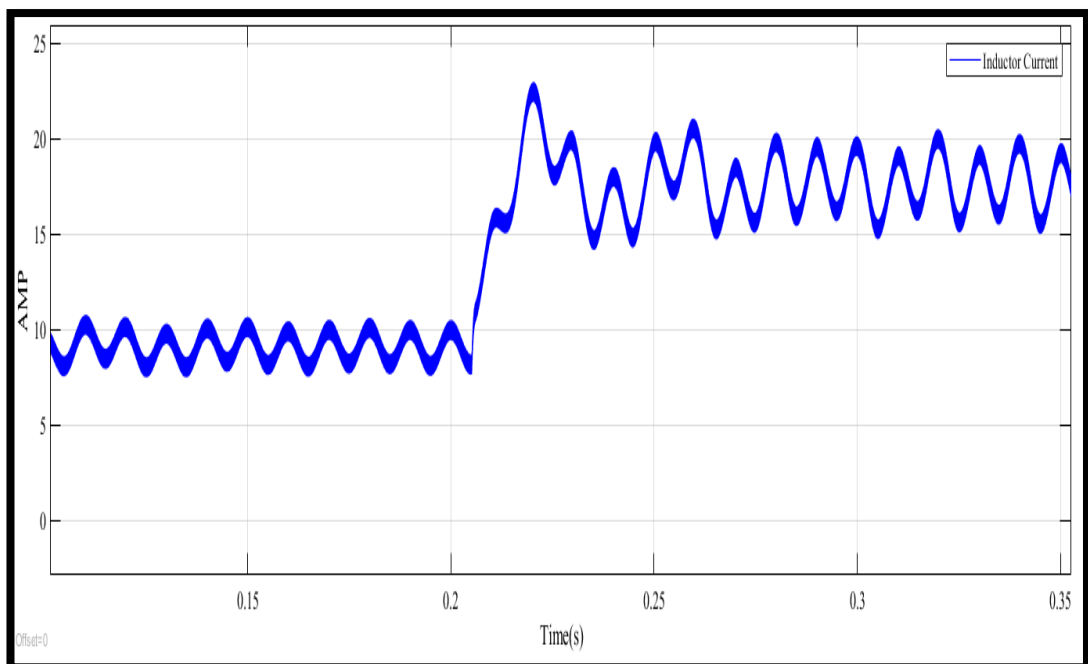


Figure 44: Inductor Current of Load Change for the New PWM Method State 1

6.2.1.2 Simulink Result of The New PWM Method state 2

State 2 shows the Simulink results for new PWM control method when $M = 0.85$, $D = 0$ and $V_{dc} = 100$.

The RMS output voltage is equal to 110V as shown in Figure 45

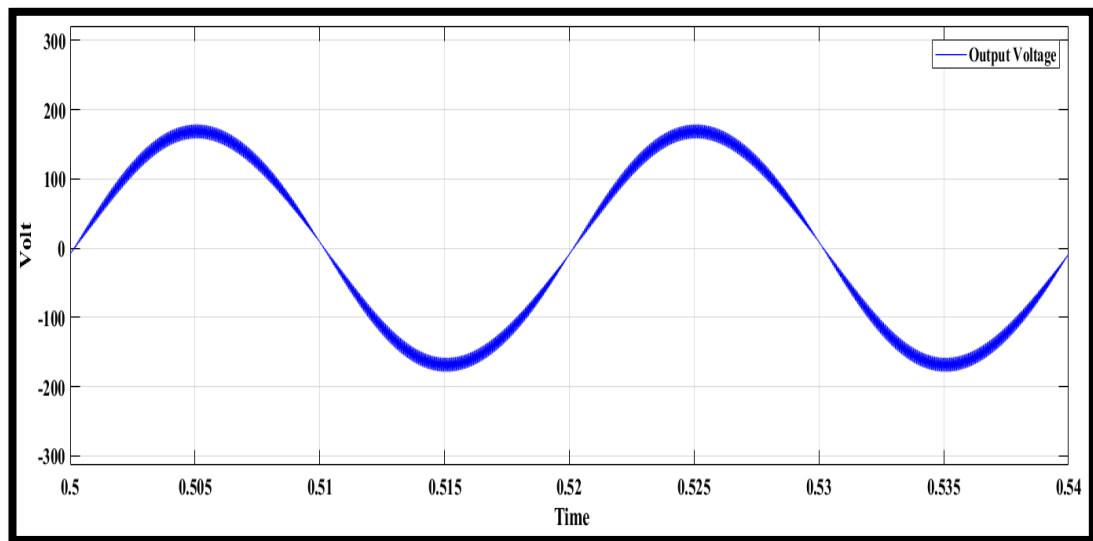


Figure 45: Output Voltage New PWM Method State 2

The peak capacitor voltage is 207V as shown in Figure 46

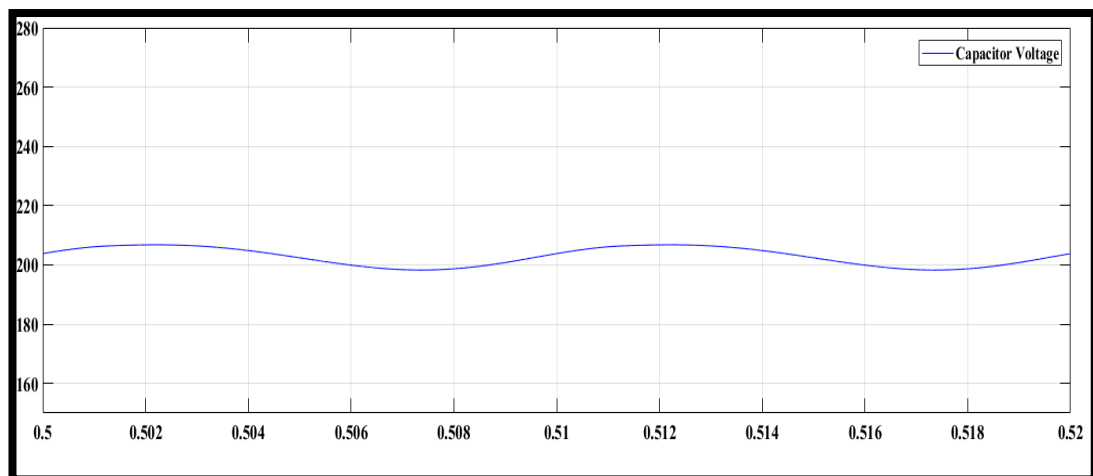


Figure 46: Capacitor Voltage of the New PWM Method State 2

The average inductor current is equal to 4A as seen in Figure 47

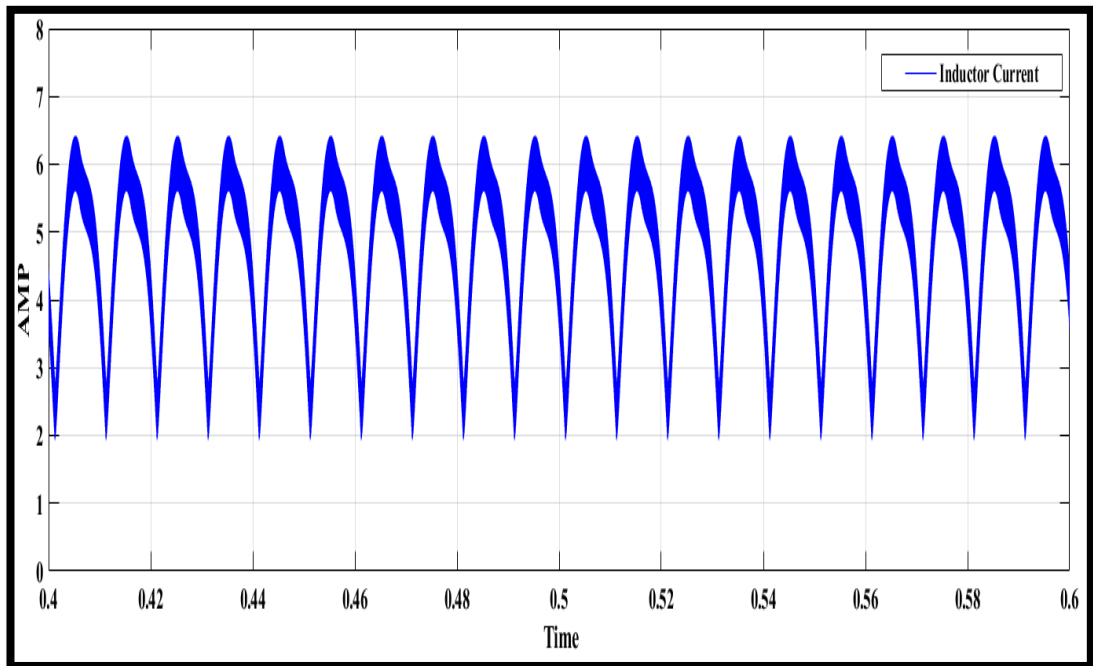


Figure 47: Average Inductor Current of the New PWM Method State 2

The high frequency peak to peak inductor current is equal to 0.9A as shown in Figure 48

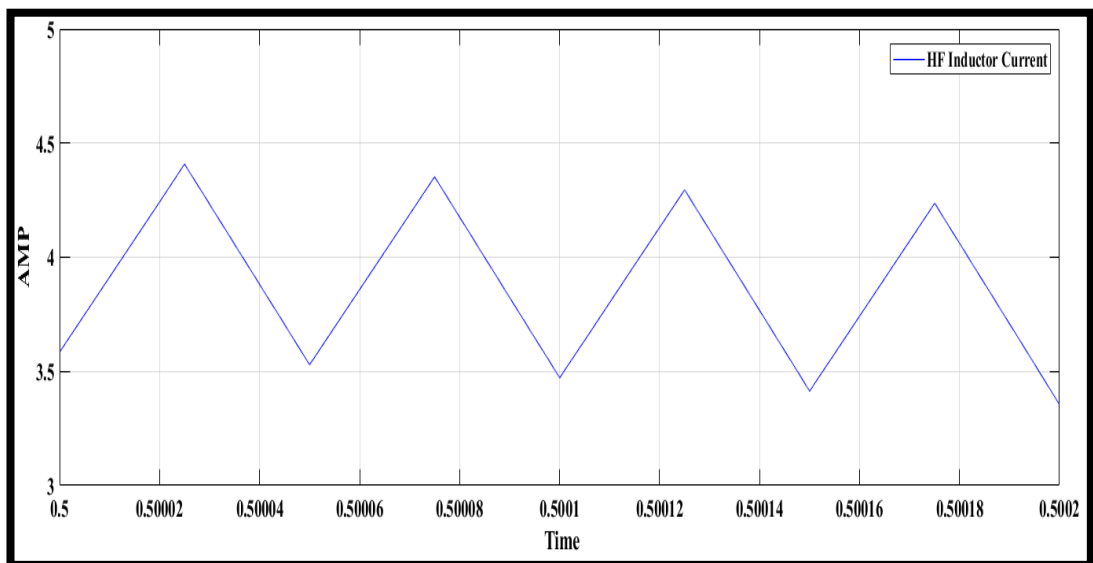


Figure 48: HF Inductor Current of the New PWM Method State 2

The high frequency peak to peak capacitor voltage is equal 1.5 as shown in Figure 49

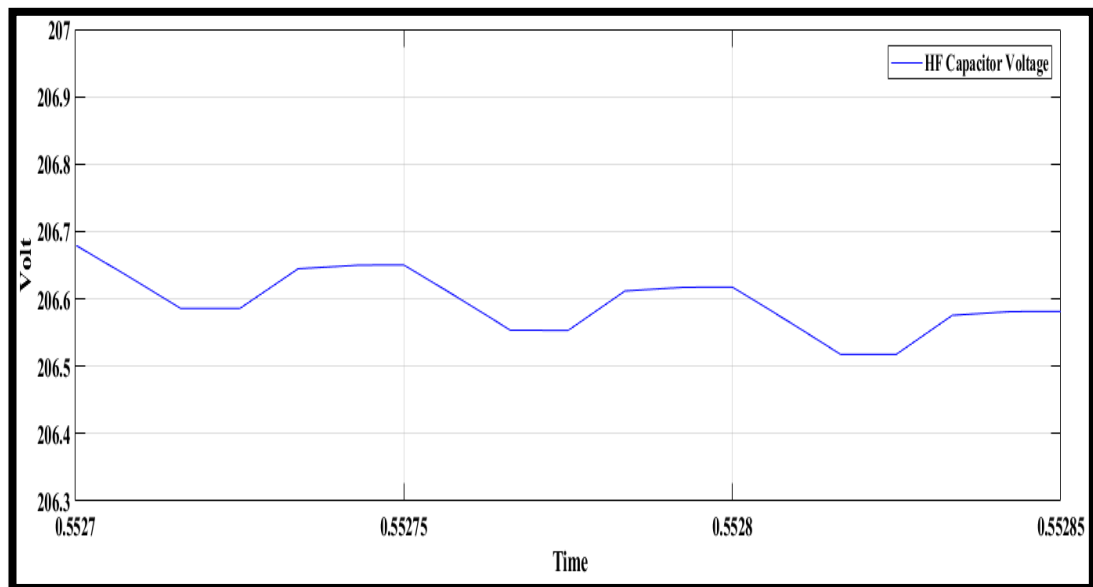


Figure 49: HF Capacitor Voltage of the New PWM Method State 2

The total harmonic distortion output current is equal to 3.2% as shown in Figure 50

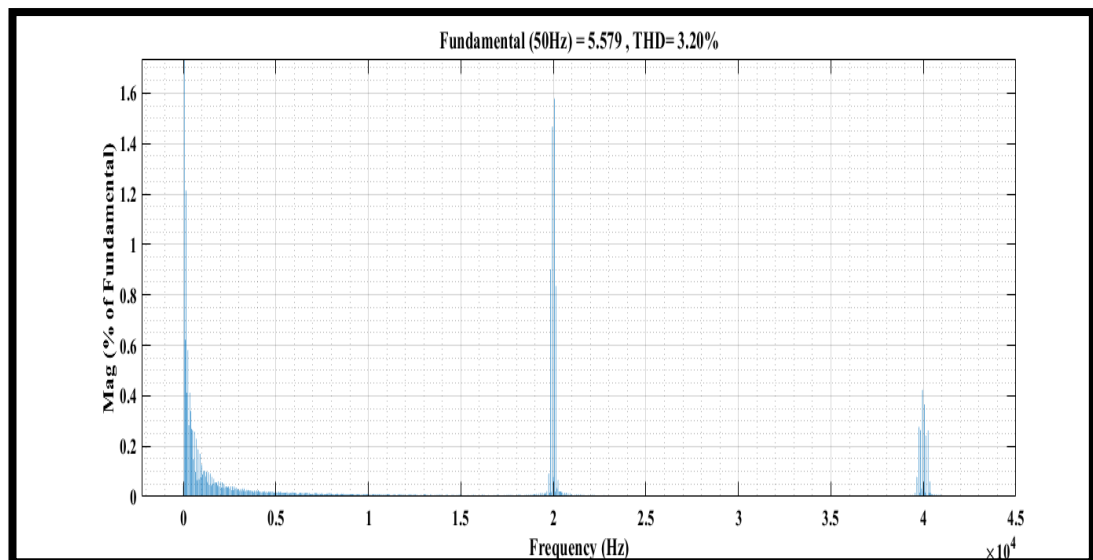


Figure 50: THD Output Current of the New PWM Method State 2

6.2.2 Simulation Result of SBC Method

Smiulink-Matlab results of the qSBI under the conventional SBC method when $M = 0.6$, $D = 0.4$ and $V_{dc} = 58$.

The RMS output voltage is equal to 110V as shown in Figure 51

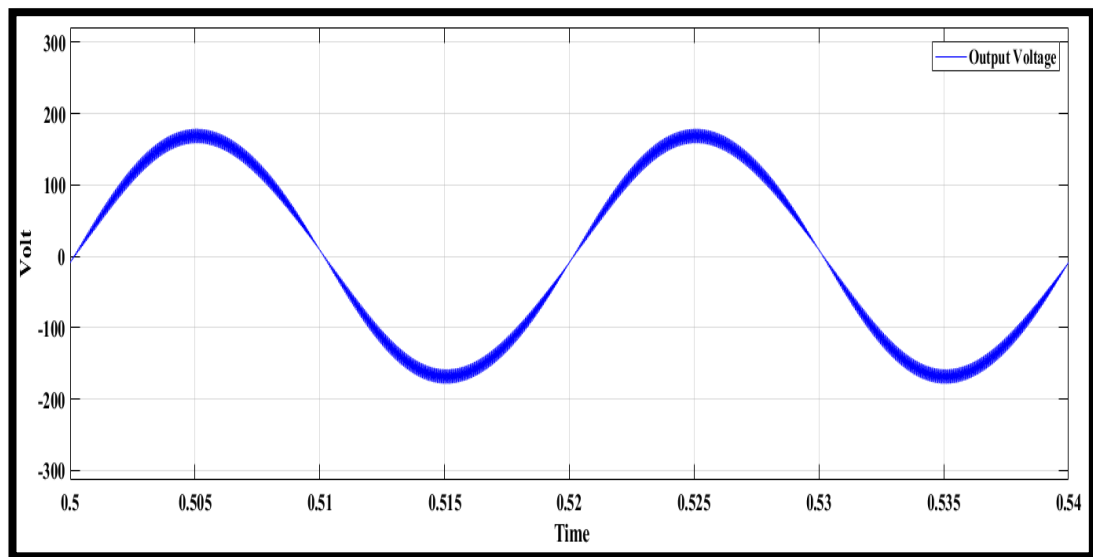


Figure 51: Output Voltage for SBC Method

The peak capacitor voltage is equal 286V as shown in Figure 52.

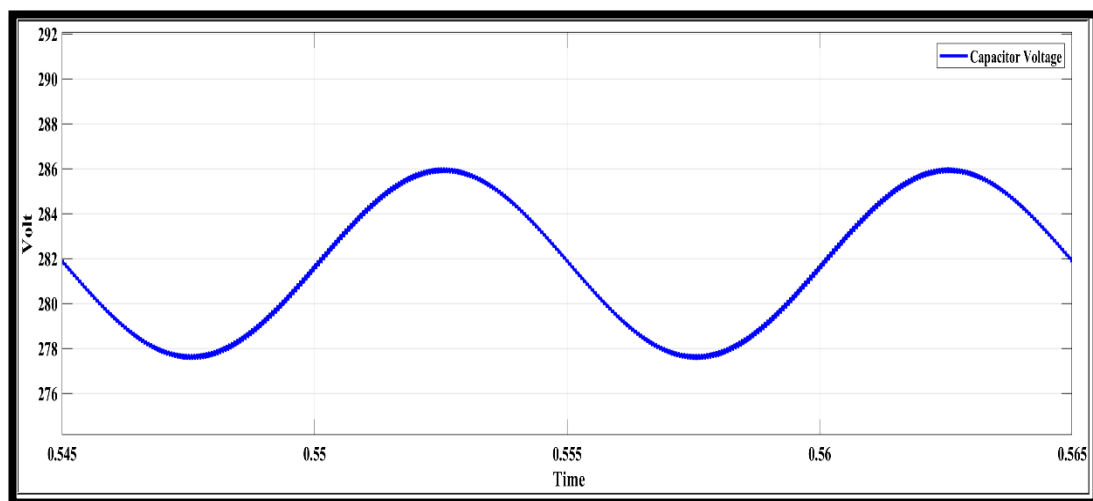


Figure 52: Capacitor Voltage for SBC Method

The peak dc link voltage is equal 286V as shown in Figure 53.

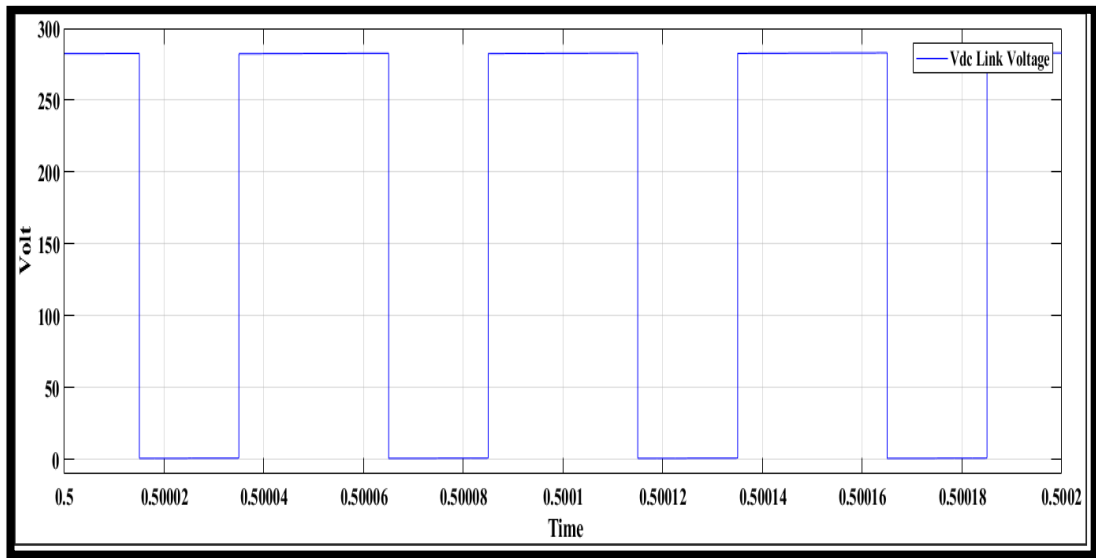


Figure 53: Dc Link Voltage for SBC Method

The high frequency peak to peak inductor ripple current is equal 2.25A as shown Figure 54.

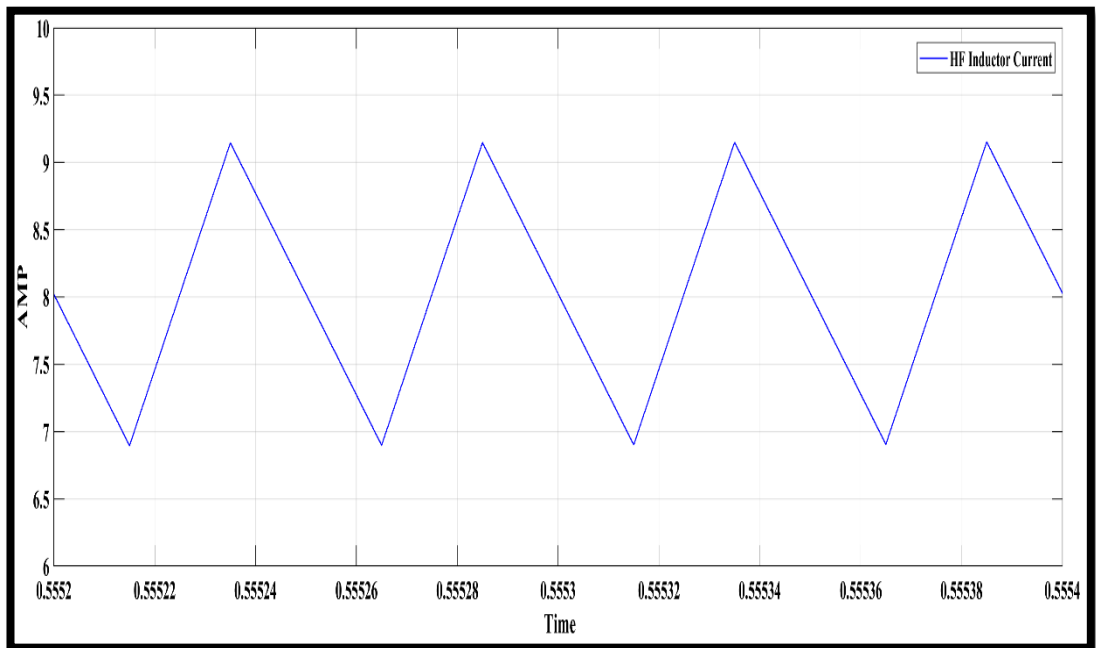


Figure 54: HF Inductor Ripple Current for SBC Method

The high frequency peak to peak capacitor ripple voltage is equal 0.24V as shown in Figure 55.

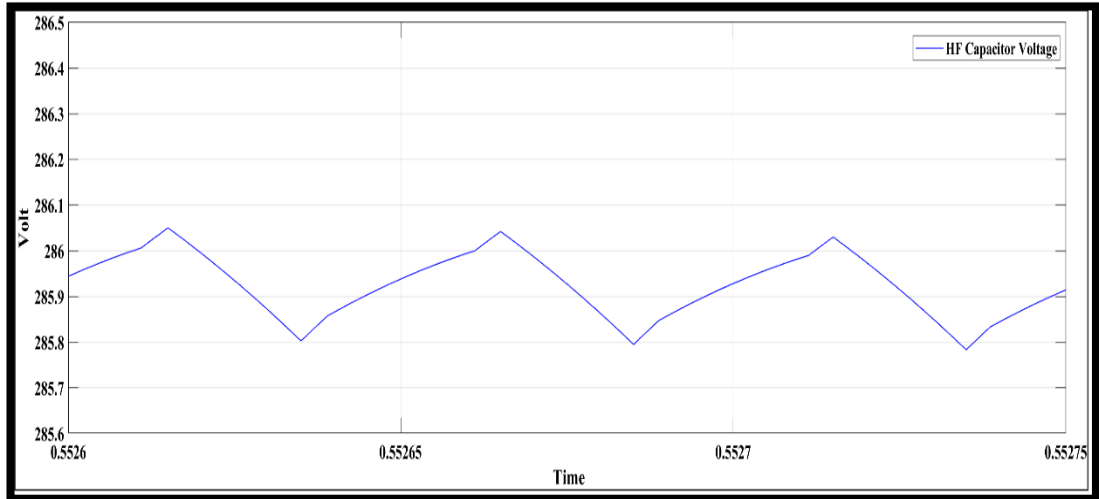


Figure 55: HF capacitor voltage for SBC Method

The average Inductor current is equal to 8.5Aits shown Figure 56

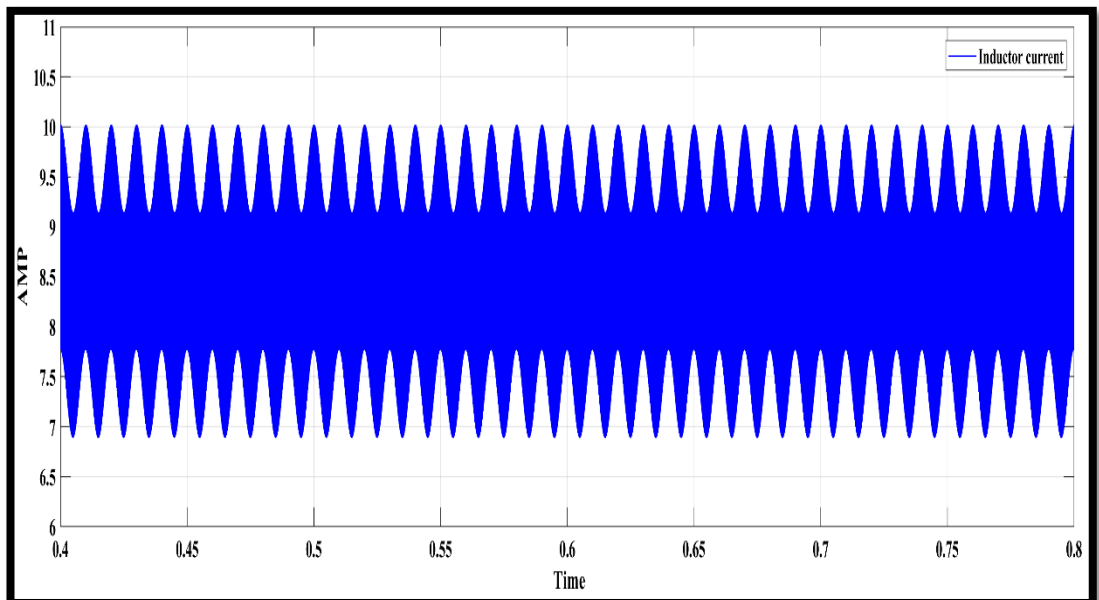


Figure 56: Inductor Current for SBC Method

The peak low frequency inductor current is equal to 0.38A as shown in

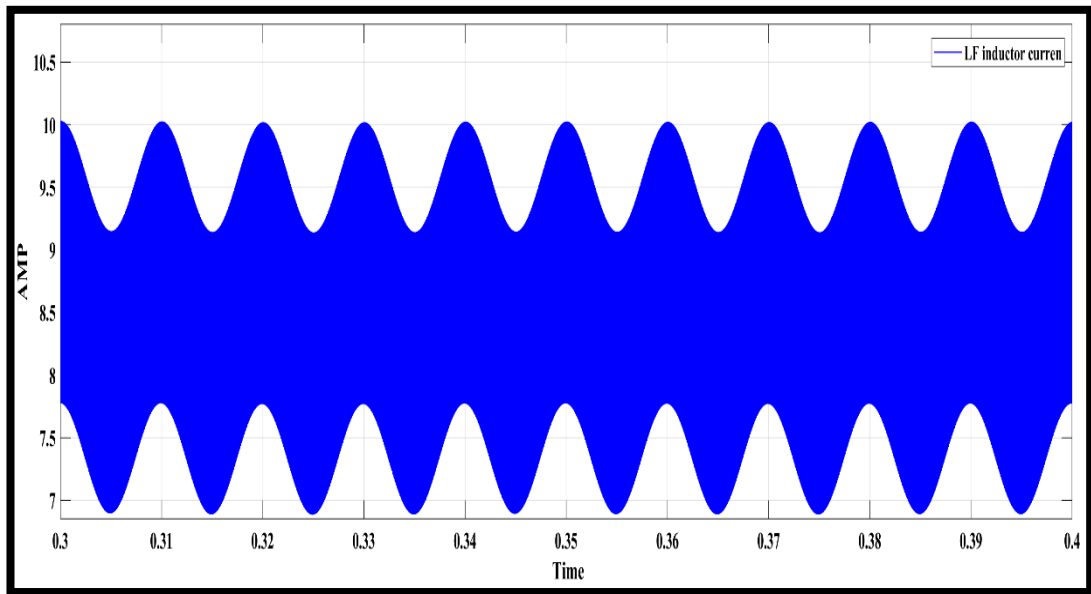


Figure 57: Low frequency Inductor Current for SBC Method

The peak low frequency of capacitor voltage is equal 4.2V as shown in Figure 58.

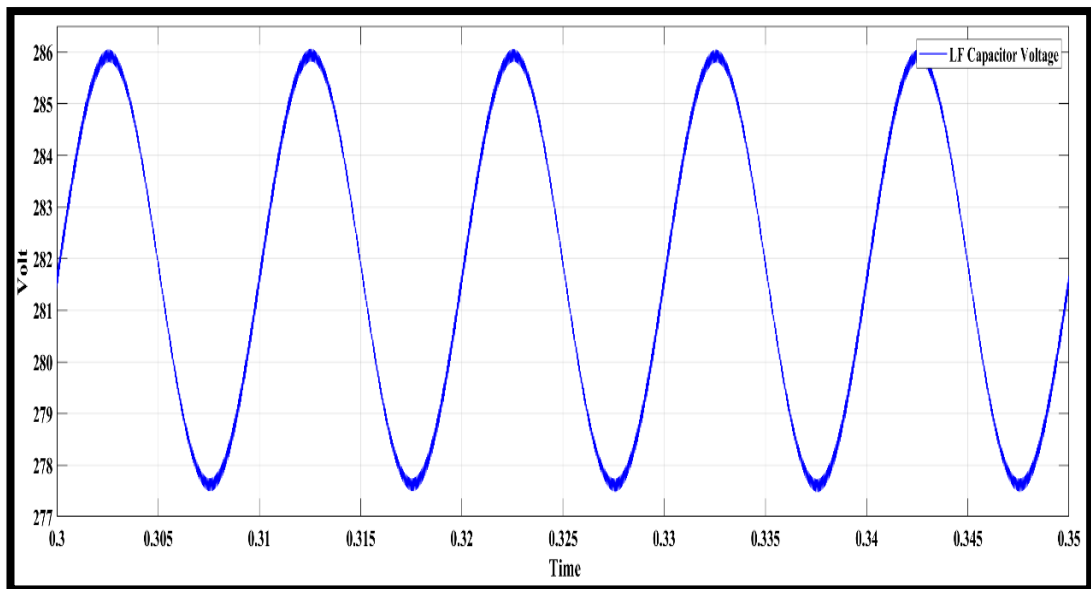


Figure 58: Low Frequency of Capacitor Voltage for SBC Method

The peak drain to source voltage of switch 5 is equal 286V as seen in Figure 59.

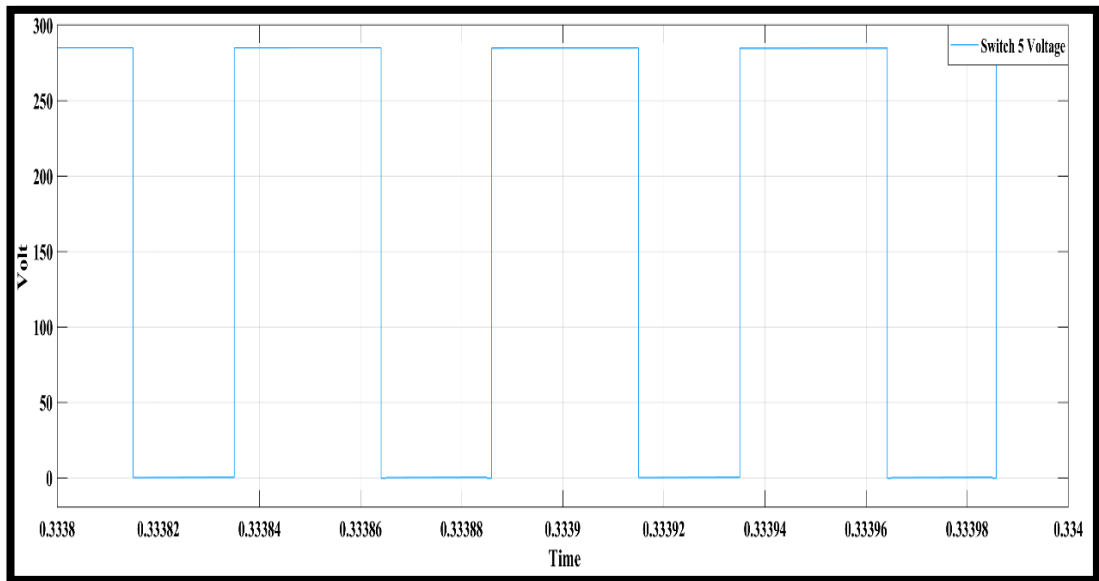


Figure 59: Switch 5 Voltage for SBC Method

The peak voltage drain to source of switch 1 is 286V as shown in Figure 60

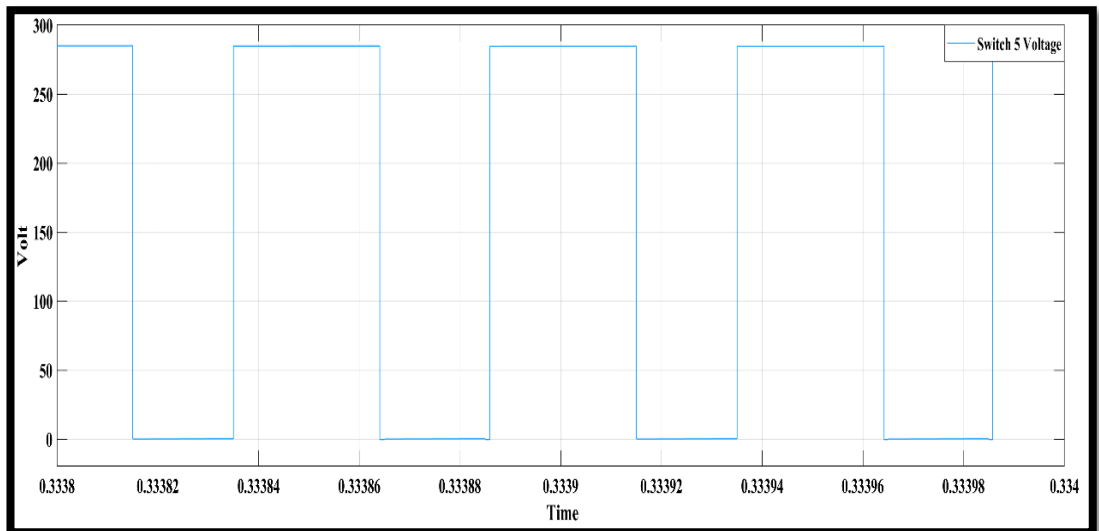


Figure 60: Switch 1 voltage for SBC Method

The RMS output current is 3.9A as shown in Figure 61.

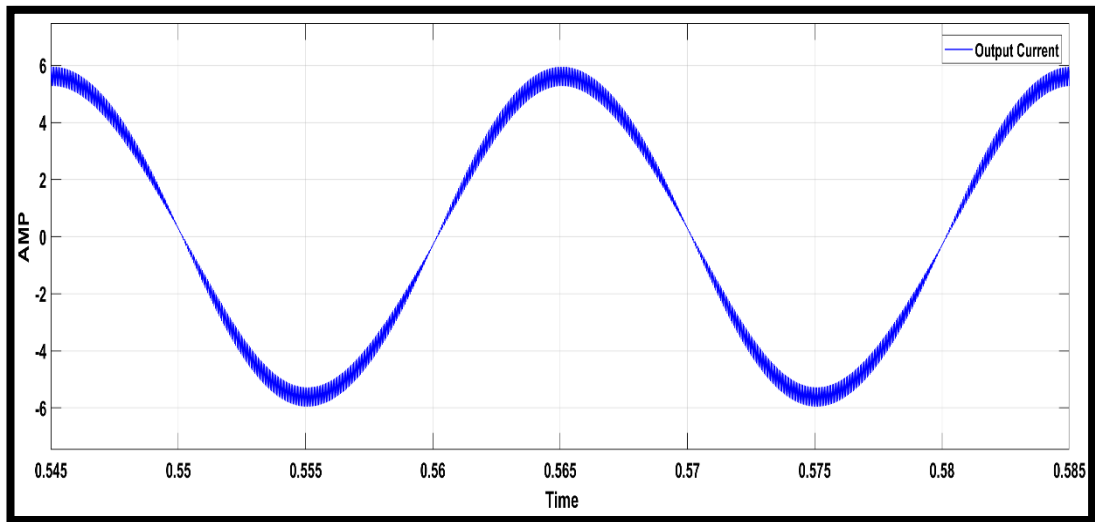


Figure 61: Output Current for SBC Method

The THD output current is equal 4.42% as shown in Figure 62.

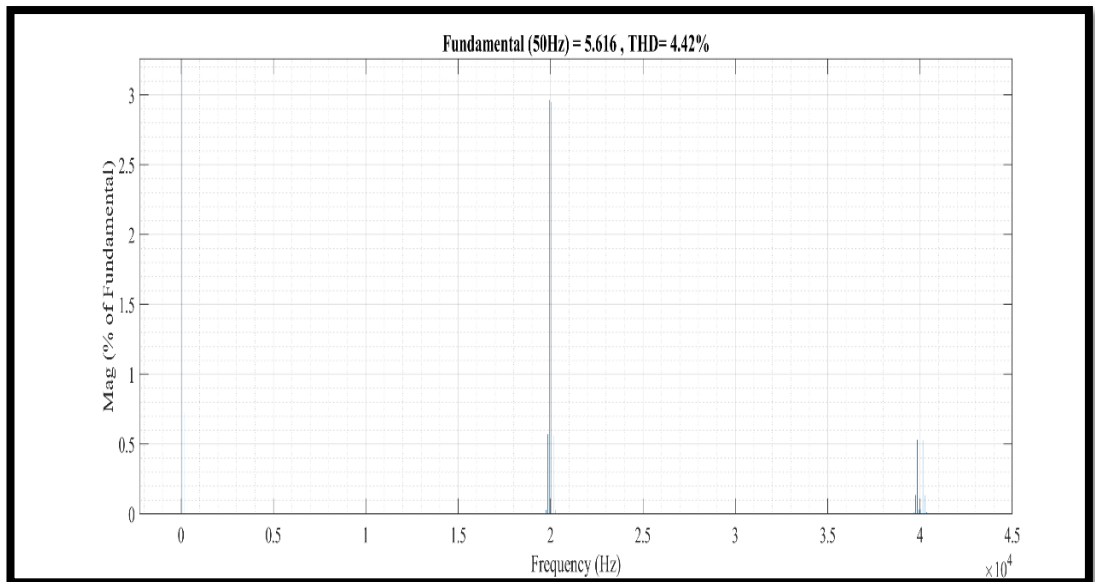


Figure 62: THD Output Current for SBC Method

6.3 Comparison between the New PWM and the Conventional SBC

Methods by Simulink Result

Table 4: Simulink Result for the New PWM Method

| | SBC | New method |
|--|------------|-------------------|
| Capacitor voltage | 286 V | 211 V |
| Switch voltage stress | 286 V | 211 V |
| Average inductor current | 8.5 A | 9 A |
| HF peak to peak inductor ripple current | 2.25 A | 1.1A |
| HF peak to peak capacitor ripple voltage | 0.24 | 0.2 A |
| Peak value of LF capacitor voltage | 4.2 V | 6 V |
| Peak value of LF inductor voltage | 0.38A | 0.88A |
| Total harmonic distortion output current | 4.42% | 3.14% |

For the same output voltage and current we recognized that the under New PWM control method the stress on devices reduced significantly also the high frequency for peak to peak capacitor voltage and inductor current decreased .

Chapter 7

CONCLUSION AND FUTURE WORK

7.1 Conclusion

The new pulse width modulation (PWM) control scheme improved the modulation index for the qSBI to improve the output voltage quality compared to the conventional SBC method for the single-phase qSBI. The new method has different advantages: it reduces the voltage stress on the diodes switch and capacitor, lowers the shoot-through current, and the HF peak to peak inductor current and capacitor voltage ripples where the capacitance and inductance can be reduced.

The drawback of the new PWM method in comparison with the SBC method is that it produces a high peak value of LF capacitor voltage and of the LF inductor current.

7.2 Future Work

The new PWM control method can be applied to a three-phase qSBI to improve the modulation index. There are disadvantages of the new PWM control method in comparison with the SBC control method including the high peak value of LF capacitor voltage and of the LF inductor current. In the future, it is recommended to use a new control method that can reduce the high peak.

The adjusted model is simulated by using Simulink Matlab and it is better to prove experimentally

REFERENCES

- [1] The Square wave output voltage for Single Phase Half Bridge Inverter. Retrieved from: <http://www.powere.dynamictopway.com/i6.htm> on Dec. 2019.
- [2] M. Abarzadeh, H. Madadi and L. Chang, "Power Electronics in Small Scale Wind Turbine Systems", 2019.
- [3] L. Ibarra, P. Ponce and A. Molina, "Generalized d-q frame PWM strategy for three-phase electric machinery", *IFAC-PapersOnLine*, vol. 48, no. 3, pp. 1-7, 2015.
- [4] D. Boroyevich, D. Zhang, and P. Ning, "A shoot-through protection scheme for converters built with SiC JFETs," *IEEE Trans. Ind. Appl.*, vol. 46, no. 6, pp. 2495–2500, Nov./Dec. 2010.
- [5] F. Z. Peng, "Z-source inverter," *IEEE Trans. Ind. Appl.*, vol. 39, no. 2, pp. 504–510, Mar./Apr. 2003.
- [6] J. Anderson and F. Peng, "A class of quasi-Z-source inverters," in *Proc. Annu. Meet. IEEE Ind. Appl. Soc.*, 2008, pp. 1–7.
- [7] J. Holtz, "Pulsewidth modulation-a survey", *IEEE Transactions on Industrial Electronics*, vol. 39, no. 5, pp. 410-420, 1992.

- [8] M. K. Nguyen, Y. C. Lim and S. J. Park, "A comparison between single phase quasi-Z-source and quasi-switched boost inverters," *IEEE Trans. Ind. Electron.*, vol. 62, no. 10, pp. 6336–6344, Oct. 2015.
- [9] M. Nguyen and Y. Choi, "PWM Control Scheme For Quasi-Switched-Boost Inverter to Improve Modulation Index", *IEEE Transactions on Power Electronics*, vol. 33, no. 5, pp. 4037-4044, 2018.
- [10] M. K. Nguyen, T. V. Le, S. J. Park, and Y. C. Lim, "A class of quasi switched Boost inverters," *IEEE Trans. Ind. Electron.*, vol. 62, no. 3, pp. 1526–1536, Mar. 2015.